AD NUMBER

AD884359

NEW LIMITATION CHANGE

TO

Approved for public release, distribution unlimited

FROM

Distribution authorized to U.S. Gov't. agencies only; Administrative/Operational use; Mar 1971. Other requests shall be referred to U.S. Army Tank-Automotive Command, Propulsion Systems Laboratory, Warren, MI.

AUTHORITY

USATAC ltr, 29 Oct 1971.

TECHNICAL REPORT NO. 11328

AN INVESTIGATION OF GAS TURBINE COMBUSTORS WITH HIGH INLET AIR TEMPERATURES
PART II: HEAT TRANSFER

MARCH 1971

U. S. ARMY TANK-AUTOMOTIVE COMMAND
CONTRACT NO.
DAAE07-69-C-0756

C. W. Owens
A. M. Mellor
by JET PROPULSION CENTER, PURDUE UNIVERSITY

TACOM
PROPULSION SYSTEMS LABORATORY
U.S. ARMY TANK AUTOMOTIVE COMMAND Warren, Michigan

UNCLASSIFIED
Security Classification

DOCUMENT CONTROL DATA - R & D

(Security classification of title, body of abstract and indexing annotation must be entered when the overall report is classified)

1. ORIGINATING ACTIVITY *(Corporate author)*
JET PROPULSION CENTER
PURDUE UNIVERSITY

2a. REPORT SECURITY CLASSIFICATION
UNCLASSIFIED

2b. GROUP

3. REPORT TITLE
AN INVESTIGATION OF GAS TURBINE COMBUSTORS WITH HIGH INLET AIR TEMPERATURES, PART II: HEAT TRANSFER

4. DESCRIPTIVE NOTES *(Type of report and inclusive dates)*
ANNUAL REPORT MARCH 1970 to MARCH 1971

5. AUTHOR(S) *(First name, middle initial, last name)*
Clifton W. Owens
Arthur M. Mellor

6. REPORT DATE	7a. TOTAL NO. OF PAGES	7b. NO. OF REFS
March 1971	94	45

8a. CONTRACT OR GRANT NO.	9a. ORIGINATOR'S REPORT NUMBER(S)
DAAE07-69-C-0756	TM-71-2
b. PROJECT NO.	
c.	9b. OTHER REPORT NO(S) *(Any other numbers that may be assigned this report)*
d.	11328

10. DISTRIBUTION STATEMENT
This document is subject to special export controls and each transmittal to foreign governments or foreign nationals may be made only with prior approval of U.S. Army Tank-Automotive Command ATTN: AMSTA-BSL

11. SUPPLEMENTARY NOTES	12. SPONSORING MILITARY ACTIVITY
	U.S. Army Tank-Automotive Command Propulsion Systems Laboratory Warren, Michigan

13. ABSTRACT

DD FORM 1 NOV 68 1473 REPLACES DD FORM 1473, 1 JAN 64, WHICH IS OBSOLETE FOR ARMY USE.

UNCLASSIFIED
Security Classification

14 KEY WORDS	LINK A		LINK B		LINK C	
	ROLE	WT	ROLE	WT	ROLE	WT
Gas Turbine Combustor Design						
Heat Transfer						
Radiation Heat Transfer						
Convective Heat Transfer						

REPORT NO. 11328

PURDUE UNIVERSITY

AND

PURDUE RESEARCH FOUNDATION

AN INVESTIGATION OF GAS TURBINE COMBUSTORS WITH HIGH INLET AIR TEMPERATURES

SECOND ANNUAL REPORT

PART II: HEAT TRANSFER

by

C. W. Owens
A. M. Mellor

Contract Number DAAE07-69-C-0756
U. S. Army Tank-Automotive Command
Warren, Michigan 48090
attn: AMSTA-BSI
Jet Propulsion Center
Purdue University
Lafayette, Indiana

March 1971

ABSTRACT

The wall temperature distribution of a combustion chamber is a function of the various heat transfer processes existing in the chamber and annulus. The basic turbulent conservation equations of mass, momentum, species, and energy are developed in an effort to provide an analytical rather than empirical method of determining the temperature distribution. However, the inclusion of radiation energy exchange using the radiative transport theory and the fact that the chamber flow is not one dimensional makes a closed form solution to the problem mathematically impossible.

The literature written prior to 1966 is reviewed in an effort to provide approximate analytical methods for determining the effects of the various modes of heat transfer on the wall temperature. Specifically, the review covers methods of evaluating radiation exchange between the chamber gases and walls, between different areas of the chamber wall, and between the chamber wall and the annulus casing. Also, the methods available for determining the effects of convective heating and cooling in the form of convective heat transfer in the absence of secondary flow, film cooling, transpiration cooling, and the effect of penetration jets are reviewed. Conclusions are drawn as to the possible areas in which considerable advancement in calculation procedures have been made since 1966.

TABLE OF CONTENTS

LIST OF TABLES

LIST OF FIGURES

NOMENCLATURE

		Units
A	Area	ft^2
A_τ	Turbulent viscosity	lbm/ft sec
A_g	Turbulent thermal conductivity	lbm-sec/ft^2
B	Constant of proportionality from Eqn. (4-61c)	-----
C	Carbon particle concentation	part/ft^3
C_{max}	Maximum carbon particle concentration in chamber	part/ft^3
C/H	Carbon to hydrogen ratio in the fuel by mass	-----
C_1'	Constant in Eqn. (4-61a)	-----
c.v.	Control volume	-----
C_1	Convective heat transfer in the chamber	Btu/hr ft^2
C_2	Convective heat transfer in annulus	Btu/hr ft^2
c_f	Friction factor	-----
c_p	Specific heat at constant pressure	Btu/lbm °K
c	Speed of light	ft/sec
c_o	Speed of light in a vacuum	ft/sec
D	Diffusion coefficient	ft^2/sec
D_p	Einstein's (1963) plug height	ft
d_A	Diameter of annulus	ft
d*	Hydraulic diameter	ft
$\dot{E}_{SLOT}$	Energy flux through a film cooling slot	Btu/ft^2 sec

		Units
E_b	Black body emissive power	Btu/hr ft^2
$\vec{\mathcal{F}}_i$	Radiation flux vector	Btu/hr ft
F	Radiation view factor	-----
f'	Glauert's (1956) nondimensional velocity	-----
$f(\lambda)$	Function of wavelength and particle size and distribution	-----
G_ν	Radiation quantity defined in Eqn. (2-22)	Btu/hr ft^2
g_i	Gravity or body force in i^{th} direction	ft/sec^2
H_ν	Radiation quanity defined in Eqn. (2-14)	Btu/hr ft
h_c	Convective heat transfer coefficient	Btu/ft^2 sec °K
h_{c_1}	Defined as = $0.0265 \frac{k}{d^*} (Re)_f^{0.8} (Pr)_f^{0.3}$	Btu/ft^2 sec °K
h_p	Planck's constant	lbm ft^2/sec
h	Specific enthalpy	Btu/ft^3
h_s'	Slot height	ft
$I_{b\nu}$	Black body emitted intensity at frequency ν	Btu/ft^2 hr steradians
I_ν	Intensity of radiation at frequency ν	Btu/ft^2 hr steradians
dI_ν	Differential change in I_ν	Btu/ft^2 hr steradians
K	Conductive heat transfer	Btu/hr ft^2
K_1	Constant in the flame emissivity Eqn., (Eqn. (3-28)	-----
K_1	Constant in Eqn. (4-61b)	-----
K_1'	Constant in Eqn. (4-64)	-----
K_1''	Constant in Eqn. (4-67)	-----
K_B	Boltzman's Constant	Btu/mole °K
K_i	Thermal conductivity	Btu/ft hr °K
L	Width of film cooling slot	ft

		Units
L_p	Einstein's (1963) plate width	ft
$\bar{\ell}$	Mean beam length	ft
ℓ	Mean free path	ft
m	Nondimensional mass flow rate through wall	-----
m_s	Nondimensional mass entrainment from the freestream	-----
$\dot{m}$	Mass flow rate	lbm/sec
$\dot{m}''_{ENT}$	Rate of mass entrainment from mainstream into the boundary layer	lbm/ft^2 sec
N_{CR}	A measure of the importance of conductive to radiative heat transfer in a system	-----
n	A measure of the rate of heat transfer and mass transfer to momentum transfer in a system	-----
Pr	Prandtl number	-----
P	Pressure	lbf/in^2
p	pressure	lbf/in^2
$\bar{p}$	Time averaged pressure	lbf/in^2
$P_v(\vec{s}-\vec{s})$	Probability function used in Eqn. (2-10)	-----
Q	Mass flow rate	lbm/sec
q_C	Conductive heat transfer flux	Btu/ft^2 sec
q_R	Radiative heat transfer flux	Btu/ft^2 sec
q_{RC}	Combined radiation and conduction heat transfer flux	Btu/ft^2 sec
q_{CO}	Convective heat transfer flux	Btu/ft^2 sec
q''_{ri}	Radiation heat transfer per unit area in the i^{th} direction	Btu/ft^2 sec
q''_v	Heat generated per unit volume	Btu/ft^3 sec
R_1	Radiation flux from the flame to the wall	Btu/ft^2 sec
R_2	Radiation flux from the combustor wall to the casing wall	Btu/ft^2 sec

		Units
R_3	Radiation flux between chamber walls	Btu/ft^2 sec
Re	Reynolds number	-----
r	Local fuel to air ratio	-----
r_{max}	Maximum radius considered for radiating hemisphere above a surface element	ft
r_s	Radius of emitting hemisphere of gas	ft
r_1	Radial length of flame element	ft
r_3	Radius of chamber	ft
St	Stanton Number	-----
s	Distance	ft
$\vec{s}$	Direction	-----
$\vec{s}'$	Direction	-----
T_{IN}	Inlet temperature to the combustor	°K
ΔT	Rise in Temperature due to combustion	°K
T	Temperature	°K
$\overline{T}$	Time averaged turbulent temperature	°K
t	Time	sec
U	Reference velocity for wall jet flow	ft/sec
u_i	Velocity in i^{th} direction	ft/sec
$\overline{u}_i$	Time averaged turbulent velocity	ft/sec
u	Velocity in x-direction	ft/sec
u_i'	Velocity of fluctuation	ft/sec
V	Volume	ft^3
v	Velocity in y-direction	ft/sec
$\overline{\dot{w}}^m$	Time averaged production rate of species m per unit volume	lbm/ft^3 sec
X	Characteristic length of system	ft

		Units
X_i	Direction	-----
X_{fw}	Distance from flame to wall element for two dimensional radiation exchange	ft
X_a	Distance from an arbitrary datum to wall element on wall a	ft
X_b	Distance from an arbitrary datum to wall element on wall b	ft
ΔX_f	Elemental length of flame	ft
X_{CO_2}	Mole fraction of CO_2	-----
X_{H_2O}	Mole fraction of H_2O	-----
y_m	Mass fraction of species m	-----
$(1-Z_E)$	Measure of magnitude of free-mixing-layer component of the velocity profile	-----
α	Thermal diffusivity $k/\rho\, c_p$	ft^2/sec
α'	Angle between $\vec{s}$ and $\vec{s}'$	Degrees
α_w	Absorptivity of the wall	-----
α_f	Absorptivity of the flame	-----
α_{WJ}	A measure of the extent of frictional effects on the flow for the velocity profile beyond the maximum velocity	-----
β	Coefficient of thermal expansion	$°K^{-1}$
β_ν	Monochromatic extinction coefficient	ft^{-1}
Γ	Transmittance of thermal radiation	-----
Γ_{mean}	Transmittance of thermal radiation evaluated at mean chamber radius	-----
δ	Boundary layer thickness	ft
δ_{BL}	Boundary layer thickness	ft
δ_{X_a}	Wall element length on wall a	ft
δ_{X_b}	Wall element length on wall b	ft
ε	Emissivity of radiating matter	-----

		Units
ε_η	Nonluminous component of emissivity	-----
ε_τ	Turbulent eddy diffusivity	lbm ft/sec
η_δ	Nondimensional distance from the wall	-----
η_ν	Monochromatic emission of matter	Btu/hr ft^2
κ_ν	Monochromatic coefficient of absorption	ft^{-1}
Λ	Luminosity factor	-----
λ_{WJ}	Function which depends on the distance from maximum velocity to the wall divided by distance from maximum to free stream velocity for the wall jet	-----
λ	Wavelength	μ
μ	Viscosity	lbm ft/sec
ν	Frequency	sec^{-1}
ρ	Density	lbm/ft^3
σ_{SB}	Stefan-Boltzman Constant	Btu/sec ft^2 °K
σ_ν	Monochromatic coefficient of scattering	-----
τ	Shear stress	lbf/ft^2
τ_o	Optical Thickness	-----
$\overline{\Phi}$	Time averaged Rayleigh dissipation term	sec^{-2}
ϕ'	Angle of inclination from normal of a surface element	Radians
ϕ	Conserved property	-----
ϕ_1	A function of r and $\overline{\ell}$	-----
ϕ_2	A function of p	-----
ϕ_3	A function of T_f or T_w in emissivity or absorptivity respectively	-----
Ω	Solid angle along $\vec{s}$	Steradians
Ω'	Solid angle along $\vec{s}'$	Steradians

Subscripts

A	Annulus
dA_1	Elemental area
dA_2	Elemental area
CA	Casing
f	Properties evalucated at the film temperature, $(T_{ms} + T_s)/2$
f	Flame, for radiation quantities
f-w	Flame to wall
G	Gas
max	Maximum value
ms	Mainstream
p	Primary zone
pc	Potential core region
s	Coolant flow through slot
TBL	Turbulent boundary layer region
w	Wall
WJ	Wall Jet region
w-c	Wall to casing
X_{CS}	Cross section at X
τ	Turbulent quantities
ν	At frequency ν

Superscripts

a	Power relating distance and velocity used by Glauert (1956)
b	Power relating distance and boundary layer thickness, Glauert (1956)

CHAPTER I

The proposed use of the gas turbine power plant for vehicular propulsion has focused interest on the temperature distribution along the combustor chamber walls. Unusually high wall temperatures are expected in certain applications due to the necessity of high combustor inlet temperatures to increase turbine efficiency and decrease specific fuel consumption; this increase in inlet temperature is the result of use of a regenerative cycle in vehicular gas turbine engines.

Due to these unusually high temperatures, an analytical approach to the determination of the wall temperature distribution is desirable for two reasons. Firstly, the presently available empirical data used for predicting wall temperature distributions will not be applicable in the high temperature ranges. Thus, it would be a significant accomplishment if theoretical results could be extended into the high temperature region. Secondly, as the wall temperatures increase, the necessity for effectively using the available coolant gases becomes more important. Therefore, the current study is concerned with possible analytical analyses of heat transfer in gas turbine combustion chambers.

This report is the first portion of a literature review which will provide an understanding of the empirical and theoretical tools available for the analysis. One such analysis has already been completed by Northern Research and Engineering Corporation (Anon., 1968) with limited useful results. Since this analysis was completed in 1966 it forms a suitable division for the present literature review. The first segment of this review concerns those articles directly used in the NREC analysis and other significant articles written before 1966. The second part of the review will deal with those works published since 1966. The latter will hopefully provide the background material necessary for understanding and judging those advancements since 1966.

The literature review of those articles written before 1966 has been completed, and the findings are reviewed herein. Preliminary to the actual review is a description of the situation which is under study. The appropriate conservation laws are developed but cannot be solved for the properties of the combustion system since the analysis is mathematically intractable. Thus, it must be replaced by an approximate method which relies on the theory of superpositioning as utilized in the Northern Research analysis.

The remainder of the report consists of a review of the analytical and empirical techniques available for prediction of wall temperature distributions. As noted previously, each of the articles reviewed was written before 1966. The three basic modes of heat exchange, convection, conduction, and radiation are covered in the forms found in the combustion chamber. The final section of the report consists of a summary of the analyses presented and some conclusions as to the direction of advancement since 1966.

Before embarking on the development of a suitable model, the connection between this portion of the gas turbine program and that discussed in Part I (Hammond and Mellor, 1971) and Part III (Anderson and Mellor, 1971) of the Second Annual Report should be made clear. The analysis of Hammond and Mellor (1970a, 1970b) provides the necessary mean gas temperature and composition along the centerline of the combustor for any heat transfer analysis. Another connection between the combustor modelling project and the heat transfer analysis is the NREC airflow and heat transfer analysis (Anon., 1968), which has been incorporated in a computer program written for NASA Lewis Research Center. This program provides the air flow distribution necessary for the determination of the mean temperature and gas composition from the combustor modelling program and as noted, its heat transfer program provides a wall temperature distribution.

Immediately the question arises as to why the NASA Lewis program cannot be used for the heat transfer analysis. The reason is that to determine the wall temperature distribution with this program, the operator must choose which modes of heat transfer are most important in the combustor chamber he is designing. The only means available at the

present time for determining whether the correct choice has been made is to compare the analytical results with experimental data for the combustor. Therefore, the program is of limited use since empirical determinations of heat transfer are still required. Clearly it is desirable to develop a purely analytical technique for heat transfer estimates, and the present study is concerned with determining if this possibility exists in view of the literature published since 1966.

In order to ascertain the validity of any advancements made in the analytical determination, the experimental results for the wall temperature distribution, to be obtained in the facility described in the final volume of this report (Anderson and Mellor, 1971) will be necessary.

In summary, the purpose here is to report on the first phase of a literature review on heat transfer in gas turbine combustion chambers. The present report is limited to the pre-1966 period and thus allows appreciation of the state of the art at the time of writing of the NASA Lewis program, as well as advances available in the literature since 1966. A later report will be concerned with post-1966 literature and the feasibility of improving existing heat transfer analysis of gas turbine combustors.

CHAPTER II

THE MODEL

A. Basic Equations

The purpose of this section is to establish the analytical methods available for modelling heat transfer in the combustion chamber. The physical phenomena of interest occurring in the chamber are defined by the turbulent flow conservation equations. The presence of recirculation and the rotational dependence of the flow will be shown to make this approach useless. The final section reviews the approximations that have been made to analytically account for the heat transfer to the combustor wall.

Figure 1 illustrates a typical combustor of turbular, tubo-annular, or annular design. For each region of the chamber presented, the primary zone, the seconary zone, the annulus flow, and the chamber wall, the laws of conservation of mass, momentum, species, and energy are applicable. Each control volume shown for the four zones (C.V.1, C.V.2, C.V.3, and C.V.4) requires a somewhat different form of the conservation equations. The equations are simply presented here because very adequate derivations exist in numerous texts (Schlichting, 1960, Bird, Stewart, and Lightfoot, 1960).

Conservation of Mass

$$\frac{\partial \bar{u}_1}{\partial x_1} + \frac{\partial \bar{u}_2}{\partial x_2} + \frac{\partial \bar{u}_3}{\partial x_3} = 0 \qquad (2\text{-}1)$$

Conservation of Momentum

$$\rho \left(\bar{u}_i \frac{\partial \bar{u}_i}{\partial x_i}\right) = - \frac{d\bar{p}}{dx_i} + \rho g_i + \frac{\partial}{\partial x_i} \left[(\mu + A_\tau) \frac{\partial \bar{u}_i}{\partial x_i}\right] \qquad (2\text{-}2)$$

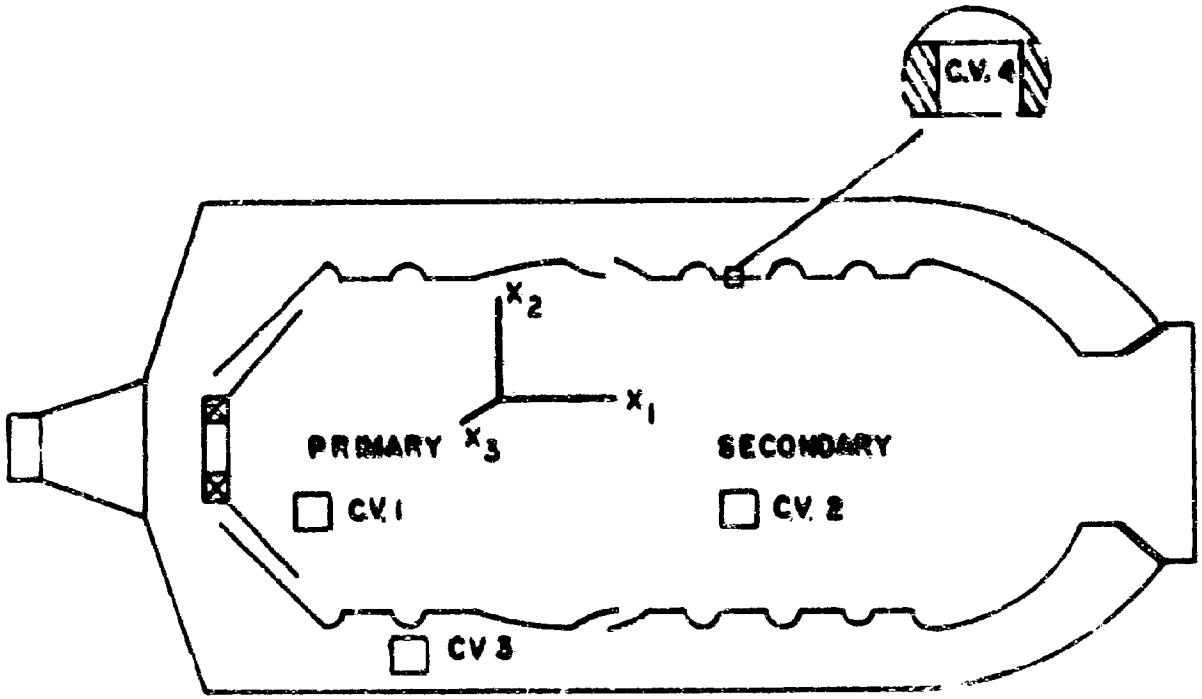

FIGURE 1 TYPICAL GAS TURBINE COMBUSTOR

Conservation of Species

$$\rho \bar{u}_i \frac{\partial \bar{y}_m}{\partial x_i} = \frac{\partial}{\partial x_i} (\rho(D + D_\tau) \frac{\partial \bar{y}_m}{\partial x_i}) + \bar{\dot{w}}'''_m \qquad (2\text{-}3)$$

Conservation of Energy

$$\rho c_p \bar{u}_i \frac{\partial \bar{T}}{\partial x_i} = \frac{\partial}{\partial x_i} [(K_i + A_g c_p g) \frac{\partial \bar{T}}{\partial x_i}] - \frac{\partial q''_{ri}}{\partial x_i} + q'''_v$$

$$+ \beta T \frac{\partial \bar{p}}{\partial x_i} + (\mu + A_\tau) \bar{\Phi} \qquad (2\text{-}4)$$

A nomenclature list is provided at the beginning of the report. The above equations are for steady, incompressible, turbulent flow.

The continuity equation for steady incompressible flow is self-explanatory. In the momentum equation, the momentum diffusion term, $\partial/\partial x_i [(\mu + A_\tau) \partial \bar{u}_i/\partial x_i]$ accounts for the laminar viscosity as well as the Reynolds stress term $\partial/\partial x_i [A_\tau \partial \bar{u}_i/\partial x_i]$. The rate of generation or destruction of species m is designated by the last term in Eqn. (2-3). For the energy equation, the term on the left hand side represents the convective transfer of thermal energy. The first term on the right hand side represents the laminar thermal diffusion plus the eddy or apparent diffusivity due to turbulence (Schlichting, 1960). The radiation exchange and the heat generation per unit volume are represented by the next two terms on the right side. The thermal expansion pressure and the viscous dissipation terms are the final terms in this equation. The dissipation term, Φ, represents the turbulent viscous heating for which the coefficient $(\mu + A_\tau)$ represents the laminar and turbulent (eddy) viscosities.

The bars over the various components indicate the time average property of the particular term. Each term consists of a time average component and a component due to the velocity of fluctuation. To cite an example, the velocity u_i is given by;

$$u_i = \bar{u}_i + u'_i$$

where $\bar{u}_i$ is the time average velocity and u'_i is the fluctuation velocity.

This term is incorporated in the dissipation function $\bar{\Phi}$ and, for momentum, in the $\partial\bar{u}_i/\partial x_i$ term associated with viscosity (Schlichting, 1960).

The four control volumes depicted in Fig. 1 are, in general, described completely by Eqns. (2-1) - (2-4) plus an equation of state. However, for all but one of these control volumes, the primary zone, it is possible to eliminate terms or one of the equations and still determine all unknowns. The process of eliminating terms will provide useful physical insight into the phenomena occurring in the zones where each control volume is situated.

For the primary zone control volume, the process of combustion requires all four of the conservation laws and an equation of state to determine the unknowns since combustion, and therefore a change in species, requires the use of the species equations to determine mass fractions of those species present. Therefore, for the primary zone all of the equations in the form stated are necessary.

As a first approximation, in the secondary zone the process of combustion can be considered to have either gone to completion or terminated. The species concentrations are unchanged by chemical reaction but still vary due to the secondary air entrainment. Although the species equation must be used, it reduces to

$$\rho\,\bar{u}_i\,\frac{\partial\bar{y}_m}{\partial x_i} = \frac{\partial}{\partial x_i}\left(\rho\,(D + D_\tau)\,\frac{\partial\bar{y}_m}{\partial x_i}\right) \qquad (2\text{-}5)$$

The cessation of the chemical processes also allows the elimination of the heat generation term, q_v''', in the energy conservation equation, Eqn. (2-4).

The final gas phase control volume, the annulus volume, C.V.3, is taken to have a constant mass fraction of oxygen and nitrogen since combustion does not occur here. The species equation and heat generation term may thus be neglected. Stemming from the low temperatures in the region and the knowledge that nitrogen and oxygen do not participate in radiation transfer (McAdams, 1954), the radiation transfer rate need not be considered in Eqn. (2-4). The existence of only two species has truncated the system of equations to four, Eqns. (2-1),

(2-2), (2-4) and an equation of state.

The final region of interest is the solid phase combustor wall or liner. Assuming the control volume in the wall is of infinitesmal axial length but of finite thickness (equal to the wall thickness) will simplify the solution to the equations. The wall is assumed to be stationary, of constant mass and chemical composition, and has no internally stored stresses or internal heat sources. If in addition body forces are neglected, Eqns. (2-1) - (2-3) are eliminated from the problem, and the energy equation is given by

$$0 = \frac{\partial}{\partial x_i}\left[(K_i + A_g C_p g)\frac{\partial \bar{T}}{\partial x_i}\right] - \frac{\partial q'''_{ri}}{\partial x_i} + \beta \bar{T}\frac{\partial \bar{p}}{\partial x_i} \qquad (2\text{-}6)$$

For most materials the thermal expansion term is small (Guy, 1959) and the material is opaque to radiation. Eqn. (2-6) may be further simplified by eliminating the turbulent conduction term, which yields the final equation:

$$0 = \frac{\partial}{\partial x_i}\left[K_i \frac{\partial T}{\partial x_i}\right] \qquad (2\text{-}7)$$

Under the assumption that the temperature is uniform normal to the wall, (in the x_2 - direction) the equation may be easily expanded.

$$\frac{\partial}{\partial x_1}\left[K_1 \frac{\partial T}{\partial x_1}\right] + \frac{\partial}{\partial x_3}\left[K_3 \frac{\partial T}{\partial x_3}\right] = 0 \qquad (2\text{-}8)$$

Note that the turbulent temperature notation has been removed because the concept of a turbulent temperature in a stationary solid has no meaning. One further assumption which has been made by Winter (1955), Lefebvre and Herbert (1960), and Tipler (1955) and followed by NREC (Anon., 1968), is that conduction in the tangential direction, x_3, is neglected. Thus, Eqn. (2-8) yields:

$$\frac{\partial}{\partial x_1}\left[K_1 \frac{\partial T}{\partial x_1}\right] = 0 \qquad (2\text{-}9)$$

The effects of radiation heating or cooling and convection appear to

be neglected in this equation. However, they are found to be included in the boundary conditions for the chamber wall control volume.

In conclusion, the equations necessary for a solution of the flow and temperature fields become increasingly more simplified as the phenomena occurring in the region decrease in number. The primary zone requires the solution of a very complicated set of equations (Eqn. (2-1)-(2-4)) involving reaction kinetics. Cessation of combustion simplifies the system of equations for the secondary zone by eliminating the chemical kinetics and the term representing an internal heat source in the energy equation (Eqn. (2-4)). Annulus flow does not require the above terms and allows the additional exclusion of radiation participation. Finally, the solid phase control volume requires only Eqn. (2-9) and two boundary conditions. The complexity of the flow makes the solution for the gas phase prohibitive, and only the solid phase control volume will be considered beyond a few concluding remarks.

An experimental investigation by Hiett and Powell (1962) indicated the recirculation zone found in a typical combustor (Fig. 2). Coupling fluid motion such as this with the induced rotational motion due to the swirlers which are present in most combustors makes the solution of Eqns. (2-1) - (2-4) impossible. For this reason, other than a theoretical heat release rate, the conditions in the gas phase have been eleminated from the analyses of Winter (1955), Lefebvre and Herbert (1960), Tipler (1955), and NREC (Anon., 1968).

Therefore, the remainder of this chapter will review the approximations made in the literature to replace the solution for the gas phase properties. The mathematically expedient process of superpositioning will be shown to approximate the solution for the wall temperature distribution and thus avoid the nonlinear integro-differential equations necessary for a mathematically exact solution. Utilizing superpositioning techniques will also separate the individual components of heat transfer into six terms, which may then be discussed separately.

B. Interaction of Radiation, Convection, and Conduction

Determination of the energy fluxes to the wall requires an under-

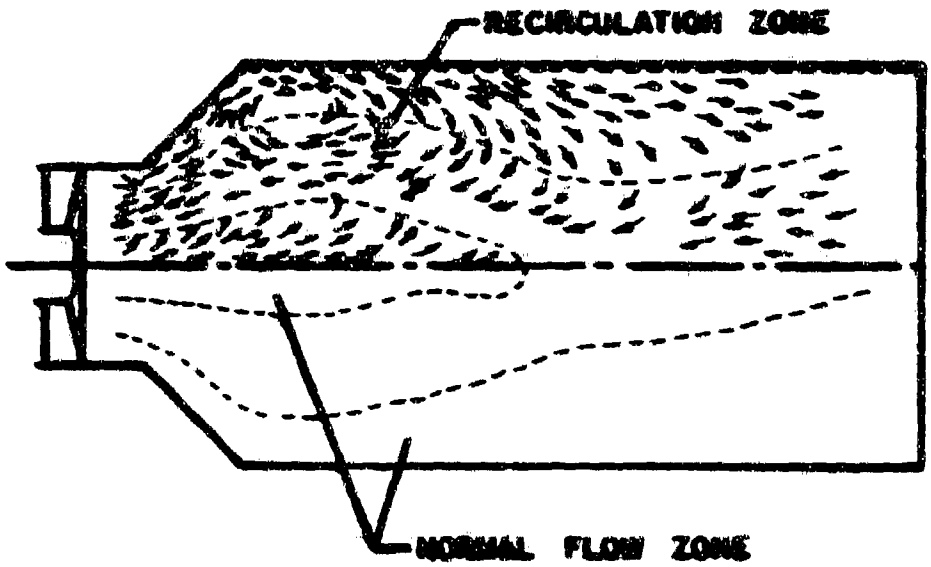

FIGURE 2 EXPERIMENTAL COMBUSTOR FLOW PATTERN (HIETT AND POWELL, 1962)

standing of radiation transport in a participating medium and its interaction with convective and conductive heat transfer. A prerequisite is thus a development of the radiative theory of transport. Viskanta (1966) developed the equation of transport on a macroscopic basis and this work shall be reviewed. Utilizing a similar development, Einstein (1963) developed the equations necessary for determining the temperature field in a flow of air through a passage including convective and conductive terms as well as radiation participation. The result of Einstein's work is the substantiation of the theory of superpositioning. Superpositioning of energy transfer modes implies that radiation, convection, and conduction are each independent of the other two contributions. The final topic of this section will be the development of the energy exchange equation for the wall using the theory of superpositioning. The exchange equation will be the basis for discussing the literature written before 1966.

Viskanta (1966) has provided a derivation of the radiation transport theory based on the physical interaction of radiation with a volume of gas. Two directions are possible for the development of the transport theory: the microscopic and macroscopic theories. Microscopic theory concerns the interaction of electromagnetic waves with the particular species present in the medium. The macroscopic theory accounts for the emission, absorption, or scattering of radiation upon interaction with a volume of gas. Emphasis must be placed on the fact that radiation is attenuated by matter and not by a volume; the study on a macroscopic basis is thus the overall interaction of radiation with the matter present. In the following, the macroscopic case has been considered. The assumptions Viskanta used are reviewed and the transport equation stated with a minimum of proof.

Several assumptions are necessary to formulate a problem which is mathematically tractable. The theory of radiation transport ignores the electromagnetic wave phenomena of interference, diffraction, and coherence, and is thus a limiting case of the more general electromagnetic theory of radiation transport. Since in order to determine the variation in temperature in the medium it is necessary to define a temperature, it is assumed that local thermodynamic equilibrium exists. Thus, non-

equilibrium radiation such as chemiluminescence is neglected. The third assumption made is that the medium is continuous and homogeneous and is capable of absorbing and emitting radiation in a coherent, isotropic manner. That is, radiation scattered by the matter in the medium does not have a preferred direction and remains at the frequency of incidence.

Consider now a cylinder of participating media which is subjected to a pencil of radiation entering through one end (Fig. 3). The ray is travelling in a direction $\vec{s}$ confined within a solid angle $d\Omega$. The monochromatic intensity, I_ν, entering the control volume is attenuated such that the intensity at the end of the control volume is $I_\nu + dI_\nu$. The change in intensity is determined by the radiation transport equation.

The radiation attenuation by absorption, scattering, and emission may be expressed mathematically. The spectral intensity of radiation at the end of the cylinder may be expressed as:

$$I_\nu \, dA \, d\Omega \, d\nu \, dt$$

Inside the volume, energy may be lost from the pencil due to absorption and scattering, which may be represented as follows

$$(\sigma_\nu + \kappa_\nu) \, I_\nu \, ds \, dA \, d\nu \, dt \, d\Omega$$

Note the inclusion of the elemental distance ds traveled along $\vec{s}$. The two coefficients are the coefficients of monochromatic scattering σ_ν and absorption κ_ν. The matter within the volume emits radiation in a frequency range from ν to $\nu + d\nu$ in the direction of $\vec{s}$, and this energy may be represented by:

$$\eta_\nu \, dV \, d\Omega \, d\nu \, dt$$

The radiant intensity is increased by radiation scattered into the volume from all possible directions which is represented by:

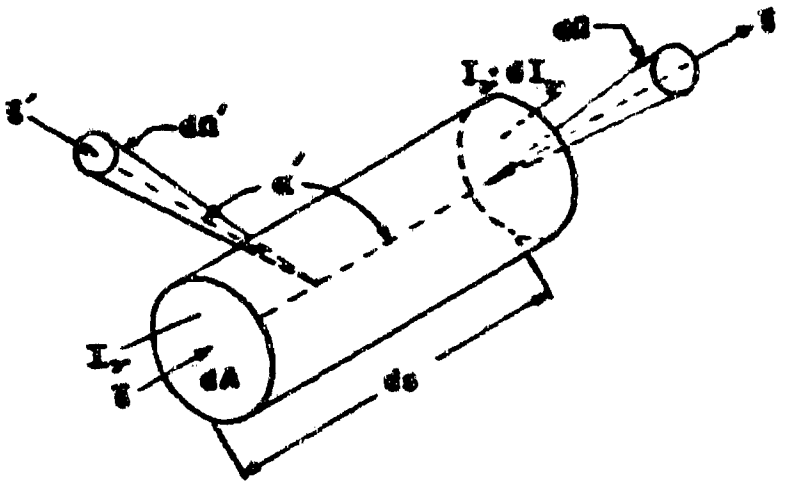

FIGURE 3 PARTICIPATING MEDIUM CONTROL VOLUME (VISKANTA, 1966)

$$\sigma_\nu \, ds \, [(1/4\pi) \int_{\Omega'=4\pi} p_\nu(\vec{s}' - \vec{s}) \, I_\nu \, (\vec{s}') \, d\Omega'] \, dA \, d\Omega \, d\nu \, dt$$

The function $p_\nu(\vec{s}' - \vec{s})$ is related to the probability of a photon entering the volume traveling along $\vec{s}'$ and being monochromatically scattered so that its final direction is $\vec{s}$. The scattering function has been normalized to unity since the probability over all directions must be unity:

$$1/4\pi \int_{\Omega'=4\pi} p_\nu(\vec{s}' - \vec{s}) \, d\Omega' = 1 \qquad (2\text{-}10)$$

The attenuation due to absorption, emission, and scattering may be formulated into an equation representing the conservation of radiant intensity over the elemental length ds in a frequency range ν to $\nu + d\nu$, in a time dt and area dA:

$$(I_\nu + dI_\nu - I_\nu) \, dA \, d\Omega \, dt \, d\nu = dI_\nu \, dA \, d\Omega \, dt \, d\nu \qquad (2\text{-}11)$$

The attenuation $dI_\nu \, dA \, d\Omega \, dt \, d\nu$ can be represented by those losses and gains mentioned above.

$$dI_\nu \, dA \, d\Omega \, d\nu \, dt = \eta_\nu \, dV \, d\Omega \, d\nu \, dt - (\sigma_\nu + \kappa_\nu) \, I_\nu \, ds \, dA \, d\Omega \cdot$$

$$\cdot d\nu \, dt + \sigma_\nu \, [(1/4\pi) \int_{\Omega'=4\pi} p_\nu(\vec{s}' - \vec{s}) \cdot$$

$$\cdot I_\nu \, (\vec{s}') \, d\Omega'] \, dA \, d\Omega \, ds \, d\nu \, dt \qquad (2\text{-}12)$$

Since dV equals dA ds, this equation may be divided by dA ds $d\Omega$ $d\nu$ dt.

$$\frac{dI_\nu}{ds} = \eta_\nu - (\sigma_\nu + \kappa_\nu) \, I_\nu + \sigma_\nu \, [(1/4\pi) \int_{\Omega'=4\pi} p_\nu(\vec{s}' - \vec{s}) \cdot$$

$$\cdot I_\nu \, (\vec{s}') \, d\Omega'] \qquad (2\text{-}13)$$

Noting that the distance ds may be represented by c dt:

$$\frac{1}{c}\frac{dI_\nu}{dt} = \eta_\nu - (\sigma_\nu + \kappa_\nu)\, I_\nu + \sigma_\nu\, H_\nu \qquad (2\text{-}14)$$

where

$$H_\nu = 1/4\pi \int_{\Omega'=4\pi} p_\nu\,(\vec{s}' - \vec{s})\, I_\nu\,(\vec{s}')\, d\Omega'$$

In actuality, the derivative of I_ν with respect to time may be replaced by the substantial derivative:

$$\frac{1}{c}\frac{DI_\nu}{Dt} = \eta_\nu - (\sigma_\nu + \kappa_\nu)\, I_\nu + \sigma_\nu\, H_\nu \qquad (2\text{-}15)$$

where, by definition:

$$\frac{DI_\nu}{Dt} = \frac{\partial I_\nu}{\partial t} + c\,\vec{s}\cdot\nabla I_\nu \qquad (2\text{-}16)$$

Therefore,

$$\frac{1}{c}\frac{\partial I_\nu}{\partial t} + \vec{s}\cdot\nabla I_\nu = \eta_\nu - (\sigma_\nu + \kappa_\nu)\, I_\nu + \sigma_\nu\, H_\nu \qquad (2\text{-}17)$$

For most engineering applications the time derivative is negligible because of the 1/c factor. Thus,

$$\vec{s}\cdot\nabla I_\nu = \eta_\nu - (\sigma_\nu + \kappa_\nu)\, I_\nu + \sigma_\nu\, H_\nu \qquad (2\text{-}18)$$

which is known as the quasi-steady radiation transport equation.

The conservation of radiant energy may be formulated using the above equation by integrating over all solid angles ($\Omega=4\pi$):

$$\int_{\Omega=4\pi} \vec{s}\cdot\nabla I_\nu\, d\Omega = \int_{\Omega=4\pi} (\eta_\nu + \sigma_\nu\, H_\nu)\, d\Omega - \int_{\Omega=4\pi} \beta_\nu\, I_\nu\, d\Omega \qquad (2\text{-}19)$$

where β_ν is the monochromatic extinction coefficient and is defined as

$(\sigma_\nu + \kappa_\nu)$. By defining a radiative flux vector $\vec{\mathcal{F}}_\nu$ as,

$$\vec{\mathcal{F}}_\nu \equiv \int_{\Omega=4\pi} \vec{s}\ (I_\nu\ d\Omega) \tag{2-20}$$

the term on the left side of Eqn. (2-19) reduces to:

$$\int_{\Omega=4\pi} \vec{s} \cdot \nabla I\ d\Omega = \int_{\Omega=4\pi} \nabla \cdot (\vec{s}\ I_\nu)\ d\Omega = \nabla \cdot \vec{\mathcal{F}}_\nu \tag{2-21}$$

The radiant energy attenuated by the medium is the second term on the right hand side and may be defined as:

$$\beta_\nu\ G_\nu = \int_{\Omega=4\pi} \beta_\nu\ I_\nu\ d\Omega \tag{2-22}$$

where,

$$G_\nu = \int_{\Omega=4\pi} I_\nu\ d\Omega$$

is the radiant energy in a frequency range ν to $\nu + d\nu$. Also,

$$\int_{\Omega=4\pi} [\eta_\nu + \sigma_\nu\ (1/4\pi) \int_{\Omega'=4\pi} p_\nu\ (\vec{s}' - \vec{s})\ I_\nu\ (\vec{s}')\ d\Omega']\ d\Omega$$

$$= \int_{\Omega=4\pi} \eta_\nu\ d\Omega + \sigma_\nu \int_{\Omega=4\pi} \int_{\Omega'=4\pi} (1/4\pi)\ p_\nu\ (\vec{s}' - \vec{s})\ I_\nu\ (\vec{s}') \cdot$$

$$\cdot d\Omega'\ d\Omega = 4\pi\ \eta_\nu + \sigma_\nu\ G_\nu \tag{2-23}$$

The probability function reduces to unity because it is integrated over all solid angles. Therefore,

$$\nabla \cdot \vec{\mathcal{F}}_\nu = 4\pi\ \eta_\nu + \sigma_\nu\ G_\nu - \beta_\nu\ G_\nu \tag{2-24}$$

which reduces to:

$$\nabla \cdot \vec{\mathcal{F}}_\nu = 4\pi\ \eta_\nu - \kappa_\nu\ G_\nu \tag{2-25}$$

One important physical implication of the above conservation of radiant

energy equation is the fact that scattering has been eliminated from the equation. This implies that scattered energy is not stored by the medium which is physically true.

The conservation of radiant energy equation may be related to the previously formulated energy equation (2-4) by replacing the $\partial q''_{ri}/\partial x_i$ term by $\partial \mathcal{F}_i/\partial x_i$ where $\mathcal{F}_i$ is the component of radiative flux in the i direction integrated over all frequencies. Thus,

$$\rho\, cp\, \bar{u}_i \frac{\partial \bar{T}}{\partial x_i} = \frac{\partial}{\partial x_i}\left[(K_i + A_g\, c_p\, g)\frac{\partial \bar{T}}{\partial x_i}\right] - \frac{\partial \mathcal{F}_i}{\partial x_i} + q'''_\nu + \beta \bar{T} \frac{\partial \bar{p}}{\partial x_i} + (\mu + A_\tau)\,\bar{\Phi} \qquad (2\text{-}26)$$

Integrating over all frequencies and noting that the emission for a medium in local thermodynamic equilibrium is given by:

$$n_\nu(T) = \kappa_\nu\, I_{b\nu}(T) \qquad (2\text{-}27)$$

where

$$I_{b\nu}(T) = \frac{2h_p \nu^3}{c_o^2\,(e^{h_p\nu/K_B T} - 1)} \qquad (2\text{-}28)$$

yields

$$\int_0^\infty n_\nu(T)\, d\nu = \int_0^\infty \kappa_\nu\, I_{b\nu}(T)\, d\nu \qquad (2\text{-}29)$$

Utilizing these equations for the variation in radiant flux along the x_i direction:

$$\rho\, c_p\, \bar{u}_i \frac{\partial \bar{T}}{\partial x_i} = \frac{\partial}{\partial x_i}\left[(K_i + A_g\, c_p\, g)\frac{\partial \bar{T}}{\partial x_i}\right] - \frac{\partial}{\partial x_i}\left[4\pi \int_0^\infty \kappa_\nu\, I_{b\nu}(T) \cdot d\nu - \int_0^\infty \kappa_\nu \int_{\Omega=4\pi} I_\nu\, d\Omega\, d\nu\right] + q'''_\nu + \beta \bar{T} \frac{\partial \bar{p}}{\partial x_i} + (\mu + A_\tau)\,\bar{\Phi} \qquad (2\text{-}30)$$

Aside from the very difficult problem of determining the necessary coefficients for the above equation, a mathematical solution in closed form would be extremly difficult to obtain except for the simpliest cases.

Einstein (1963) noted that the effects of radiation and conduction could be accounted for by superimposing the energy transport due to each of the modes in the absence of the other. The system considered is shown in Fig. 4. The effects of absorption of the gas in such a convective, conductive system was studied utilizing an equation very similar to Eqn. (2-30) but for laminar flow:

$$4k\,\sigma_{SB}\,T^4\,(\vec{R}) + \rho\,u\,c_p\,\frac{\partial T(\vec{r})}{\partial x}\Big/_{\vec{r}=\vec{R}_o} - K\,\frac{\partial^2 T(\vec{r})}{\partial y^2}\Big/_{\vec{r}=\vec{R}_o}$$

$$= k \iiint \sigma_{SB}\,T^4\,(\vec{r})\,f(\vec{r}' - \vec{R}_o)\,d\tau$$

$$+ k \iint \sigma_{SB}\,T_s^4\,(\vec{r})\,g(\vec{r} - \vec{R}_o)\,dA \qquad (2\text{-}31)\star$$

The definitions of the individual terms as presented by Einstein are given in Table 1. Einstein used Eqn. (2-31) to determine the temperature distribution in the channel for a constant wall temperature. In order to solve the integro-differential equation, it was necessary to replace the differentials with approximate finite differences in temperature between discrete zones in the flow. A grid of one hundred units was used. In this manner he was able to determine the heat transfer between the two plates and the temperature profile between the plates.

Upon analyzing the effects of radiation and conduction in the absence of convection, the total heat transferred was slightly greater than the heat transferred by conduction in the absence of radiation summed with the heat transferred by radiation in the absence of conduction. This implies that the total heat transfer may be approximated

---

$\star$Note: The nomeclature for Eqn. (2-31) is defined in Table 1.

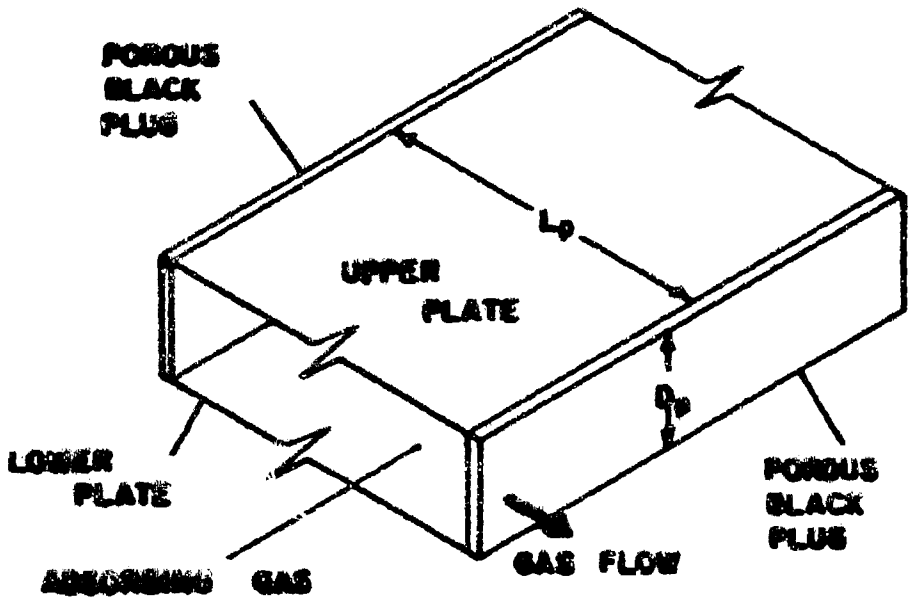

FIGURE 4 EXPERIMENTAL SYSTEM OF EINSTEIN (1963)

Table 1.

Terms in the Einstein (1963) Energy Equation

Term	Description
$4k\,\sigma_{SB}\,T^4(\vec{R}_o)$	Radiant energy emitted per unit volume at $\vec{r} = \vec{R}_o$
$\rho\,u\,c_p\,\frac{\partial T(\vec{r})}{\partial x}\Big/_{\vec{r}=\vec{R}_o}$	Enthalpy increase per unit volume of the flowing gas at $\vec{r} = \vec{R}_o$
$K\,\frac{\partial^2 T(\vec{r})}{\partial y^2}\Big/_{\vec{r}=\vec{R}_o}$	Net conduction heat transfer into the unit volume
$k \iiint \sigma_{SB}\,T^4(\vec{r})\,f(\vec{r}-\vec{R}_o)\,d\tau$	Radiation absorbed per unit volume at R_o from emission given off by surrounding gas
$k \iint \sigma_{SB}\,T_s^4(\vec{r})\,g(\vec{r}-\vec{R}_o)\,dA$	Radiation absorbed per unit volume at R_o from emission of flat plates and end surfaces

Einstein's Nomenclature

$k \equiv$ radiation absorbtion coef. of gas

$\vec{R} \equiv$ position vector of variable point in channel or surface

$\vec{r} \equiv$ position vector of variable point in channel or surface

$d\tau \equiv$ infinitesimal volume element in gas

$f(\vec{s}) \equiv$ gas-line-source to gas radiation exchange factor

$g(\vec{s}) \equiv$ surface-line source to gas radiation exchange factor

Subscripts

$s \equiv$ surface

$o \equiv$ integrated mean conditions at channel outlet

by the summation of the individual components acting independently of each other:

$$q_{RC} = q_R + q_C \qquad (2\text{-}32)$$

The accuracy of this assumption is exhibited in Fig. 5; $q_{RC}/(q_R + q_C)$ is plotted against the optical thickness τ_o for various values of $N_{CR} \equiv K/Dp\ \sigma_{SB}\ T^3$, which is a measure of the importance of conduction compared to radiation in the system.

Einstein's results indicate that the approximation is most accurate for the two limits of an optically thick or thin medium (the optical thickness is a measure of the mean free path of a photon in the system). As would be expected, for heat transfer when conduction ($N_{CR} = 2.08$) or radiation ($N_{CR} = 0.0208$) is dominant, the approximation has a maximum error of 4%. When both modes influence the heat transfer ($N_{CR} = 0.104$ or $N_{CR} = 0.208$) the error is a maximum at 9%. Viskanta and Grosh (Cess, 1964) utilizing a similar physical system found that the maximum error was 11%. Again, the discrepancy was greatest for systems which had significant radiation and convection.

An extension of the above example of superpositioning has been utilized by Winter (1955), Lefebvre and Herbert (1960), and Tipler (1955). Rather than considering the system of equations (2-1) - (2-4) for each of the gas control volumes to determine the boundary conditions for Eqn. (2-9), the solid control volume equation, the process of heat transfer has been approximated as the summation of the individual components of heat transfer acting as if the other components were not present.

Fig. 6 illustrates the analysis of Tipler (1955) using the concept of superpositioning. The radiant heat flow from the flame to the combustion chamber wall is represented by R_1.* The radiant exchange between the walls at high temperature (in the primary zone, for example) to the walls at lower temperatures (in the secondary zone) is designated by R_3. The chamber walls will also increase in temperature due to the

*The notation used herein is attributed to Winter (1955).

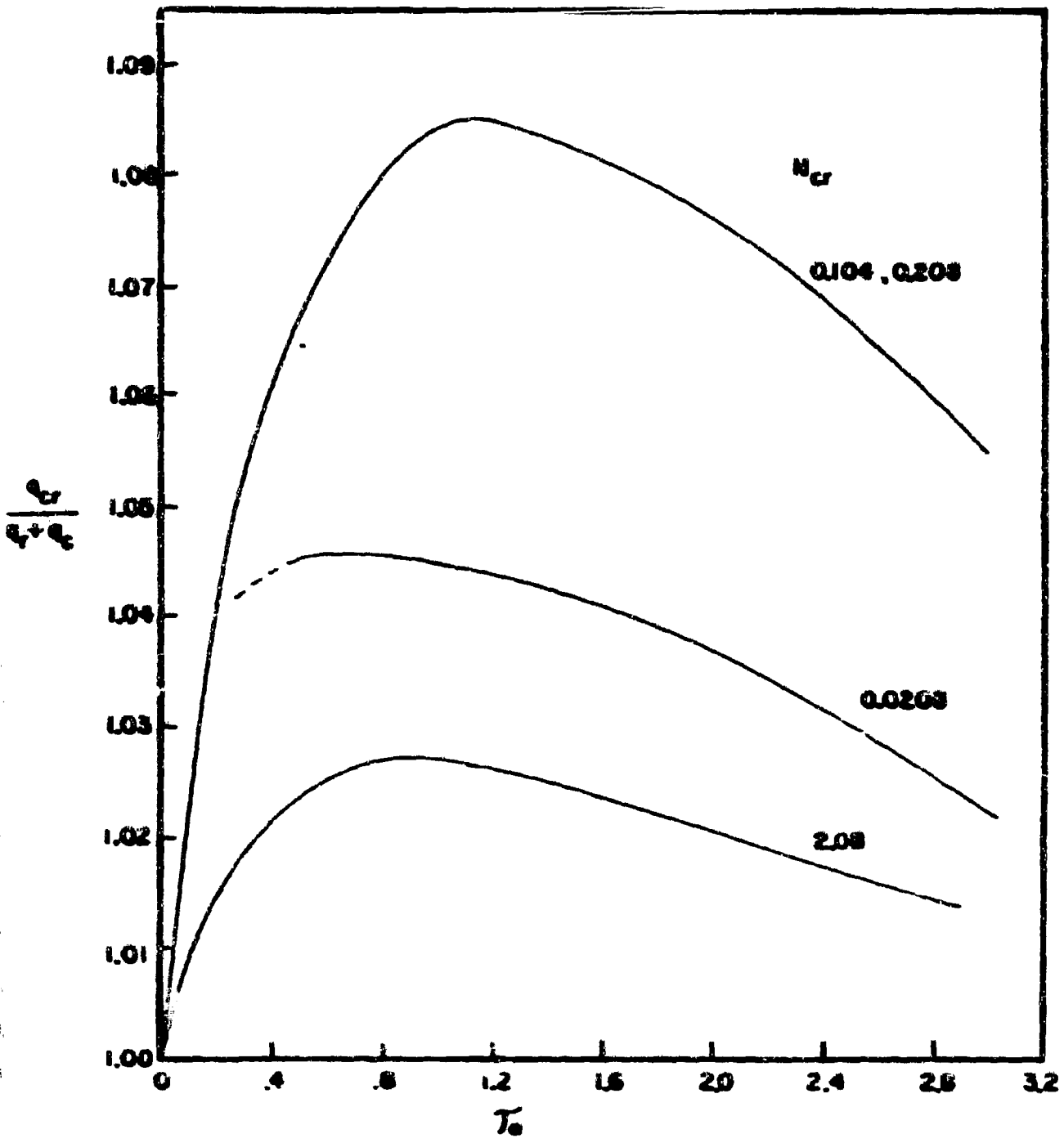

FIGURE 5 ERROR IN APPROXIMATING THE CONTRIBUTIONS OF RADIATION AND CONDUCTION USING THE SUPERPOSITION METHOD (EINSTEIN, 1963)

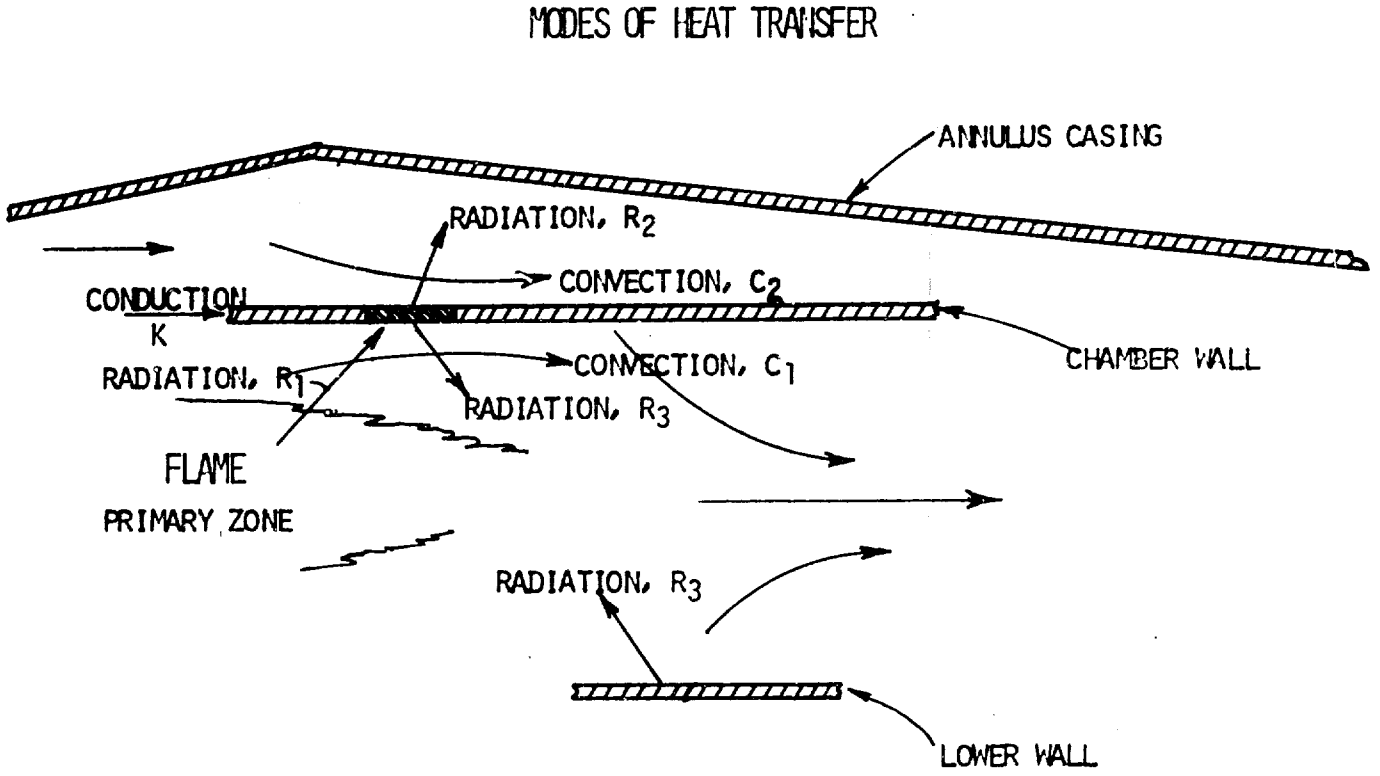

FIGURE 6 TIPLER'S MODEL OF HEAT TRANSFER COMPONENTS

convective heating of the hot combustion gases represented by C_1. Assuming for the moment that the wall is insulated, the heat transfer to a wall element may be calculated in the following manner:

$$K + R_1 + C_1 = R_3 \tag{2-33}$$

The sign of K, the conduction component, is dependent on the gradient of the temperature as defined by Fourier's law of heat conduction (McAdams, 1954):

$$K = K_i \frac{\partial T}{\partial x_i} \tag{2-34}$$

In the instance of secondary air flow through the annulus, heat will be lost from the wall by convection and radiation (Tipler, 1955) since the annulus gases are at a lower temperature than the combustion products in the chamber. The convective cooling component of the annulus gases is specified by C_2. Three other convective cooling methods could be present in a typical combustor: penetration jets, film cooling slots, and transpiration cooling. At present these deviations from the flat-plate-type convective cooling C_2 will be neglected. Radiation exchange R_2 is also present in the annulus in the form of radiation transfer between the chamber wall and the chamber casing. The annulus terms may be considered losses from the wall element:

$$R_1 + C_1 + K = R_3 + C_2 + R_2 \tag{2-35}$$

The remainder of this report deals with the investigation of each of the terms in Eqn. (2-35), and the permutations found in typical combustors. In the next chapter, radiation in the chamber and annulus is considered, and the appropriate methods presented in the literature of interest are reviewed, for the most part, in an order of increasing approximation or dependence on empirical results. In Chapter IV the theories available for predicting the magnitude of each of the convective terms are presented. Throughout the report, discussion of empirical results has been kept to a minimum and the emphasis is placed on

theoretical developments, since an analytical model is desired.

CHAPTER III

RADIATION TRANSFER IN COMBUSTION CHAMBERS

A. Introduction

Radiation transfer in furnaces has been studied on an empirical and limited theoretical basis for many years (Lefebvre, 1965). However, only since 1960 have the theories of absorption and emission by a medium been applied to engineering rather than astrophysics problems (Cess, 1964). The result of this theory, the equations of radiation transport (Eqn. (2-18)) and the conservation of radiant energy (Eqn. (2-25)), are unfortunatly restricted by their mathematical complexity. This leads directly to the discussion of two approximate methods, the one dimensional and two dimensional formulae for flame radiation. Also necessary for the determination of flame radiation is a method for calculating the emissivities and absorptivities of the flame. The correlations available for these calculations, for both luminous and nonluminous flames, will be covered in the second section. The final two topics covered in this chapter are the evaluation of R_2 and R_3, the exchange between the wall of the chamber and the casing and the exchange between different surface areas on the inside of the chamber, respectively.

B. Flame Radiation

Of the work related to the determination of heat transfer in the combustion chamber, a great deal has been devoted to the study of radiant exchange between the flame and surroundings (Lefebvre and Herbert, 1960). Unfortunatly, a large portion of this work concerns the development of experimental techniques for investigating this phenomenon. The two methods of calculating the magnitude of R_1 which have been presented in the literature depend substantially on empirical results for accuracy. Both of the formulations and their restrictions are discussed in detail

below. The final topic of interest in flame radiation is an understanding of the empirical results and correlations of these results used to determine flame emissivities for both nonluminous and luminous flames.

The one dimensional exchange of radiation between the flame and the wall at the same axial position as the flame was first applied to aircraft combustion chambers by Winter (1955). Emphasis must be placed on the fact that the analysis is applicable to two dimensional flame radiation (that is, radiation exchange between the flame element and the wall at all axial positions) only under the assumption of a constant wall temperature (McAdams, 1954). For the case considered here, the exchange is limited to elements of the flame and isothermal elements of the wall at the same axial position. If sufficiently small wall elements are considered the area is indeed isothermal.

Utilizing the formulation for the thermal radiant emission from a black body:

$$E_b = \sigma_{SB} T^4 \qquad (3\text{-}1)$$

the energy arriving at the wall due to radiation is proportional to the difference between the energy emitted from the flame and the energy radiated from the wall which is absorbed by the flame.

$$R_1 \sim [\varepsilon_f \sigma_{SB} T_f^4 - \alpha_f \sigma_{SB} T_w^4] \qquad (3\text{-}2)$$

The coefficients ε_f and α_f represent the emissivity and absorptivity of the flame, respectively. Eqn. (3-2) is derived for the specific case of a chamber wall which is black, $\varepsilon_w = 1.0$. To account for walls which are not black and reflect radiation, an additional factor ε' has been incorporated into the equation (McAdams, 1954). The factor accounts for radiant energy which after leaving the flame has been reflected back through the flame and is absorbed or rereflected by the wall on the opposite side of the flame. Empirical results (McAdams, 1954, Winter, 1955) have indicated that:

$$\varepsilon' = \frac{(1 + \varepsilon_w)}{2} \qquad (3\text{-}3)$$

satisfactorially accounts for the multiple reflections encountered in the chamber.

Lefebvre and Herbert (1960) have found that over a wide range of optical thicknesses the absorptivity and emissivity of the flame are related by the following

$$\frac{\alpha_f}{\varepsilon_f} = \left(\frac{T_f}{T_w}\right)^{1.5} \qquad (3\text{-}4)$$

In the limit of flame and wall temperature equality, $\alpha_f = \varepsilon_f$ as would be expected from Kirchoff's law (McAdams, 1954). Eqn. (3-3) and (3-4) may be substituted into the equation for the flame radiation to give:

$$R_1 = \left(\frac{1 + \varepsilon_w}{2}\right) \varepsilon_f \sigma_{SB} T_f^{1.5} (T_f^{2.5} - T_w^{2.5}) \qquad (3\text{-}5)$$

which is explicitly valid for the one dimensional case or two dimensional case under the restrictions outlined previously.

Two values are still necessary for the calculation of R_1. In the above formula, radiant energy does not appear to be dependent on the geometry of the system. However the geometric factor is found in the determination of flame emissivities, which will be discussed in detail after the second method of calculation is reviewed. A second restriction to immediate calculation is the determination of the flame temperature. A mean temperature for the flame is usually determined from the temperature rise due to combustion over the inlet temperature, T_{IN}:

$$T_f = T_{IN} + \Delta T \qquad (3\text{-}6)$$

The value of ΔT may be determined from standard temperature rise curves based on the local fuel to air ratio (Lefebvre and Herbert, 1960).

Neglecting the radiation from a flame element to a section of the wall other than the section at the same axial location has obvious physical disadvantages. For this reason, Hottel (McAdams, 1954)

extended the one dimensional analysis to account for exchange between the flame and all sections of the wall and removed the restriction of constant temperature along the wall. Hottel began by specifying the analysis necessary for determining the shape of the gas volume.

If a hemisphere of gas is considered to be radiating at a rate $\sigma_{SB}\ \varepsilon_G\ T_G^4$ to a surface element at the base of the hemisphere, the emission from an element at radius r_s to the element per unit area, per unit of shell thickness is (see Fig. 7):

$$\frac{d(\sigma_{SB}\ \varepsilon_G\ T_G^4)}{dr_s} = \sigma_{SB}\ T_G^4\ \frac{d\varepsilon_G}{dr_s} \qquad (3\text{-}7)$$

The irradiation incident on the surface per unit thickness of the shell, dr_s, is the radiant emission divided by a factor of π:

$$dI = \left[\frac{\sigma_{SB}\ T_G^4}{\pi}\ \frac{d\varepsilon_G}{dr_s}\right] dr_s \qquad (3\text{-}8)$$

Utilizing the differential exchange between the volume and the elemental surface area,

$$dR_1 = dI\ dA \cos\phi\ d\Omega = \left[\frac{\sigma_{SB}\ T_G^4}{\pi}\right] dA\ d\Omega \cos\phi\ \frac{d\varepsilon_G}{dr_s}\ dr_s \qquad (3\text{-}9)$$

Integration over all of the volume and for the base area yields:

$$R_1 = \int_A \int_0^{r_{max}} \int_{\Omega=4\pi} \cos\phi\ d\Omega\ \frac{d\varepsilon_G}{dr_s}\ dr_s\ dA \qquad (3\text{-}10)$$

The integration of the above is a tedious procedure due to the required determination of $\cos\phi\ d\Omega$ for the geometry considered. A similar and simpler procedure was employed to determine the mean beam length $\bar{\ell}$ such that the radiant energy emitted over the entire volume is equal to the average rate of emission times the mean beam length. The value of $\bar{\ell}$ was found to depend on the partial pressure of the participating gas, P_G, times a characteristic length X. This dependence is almost a constant function of the value of X, which has been determined for certain geometries of interest (McAdams, 1954).

Hottel has shown, utilizing Eqn. (3-7), that the emission per unit

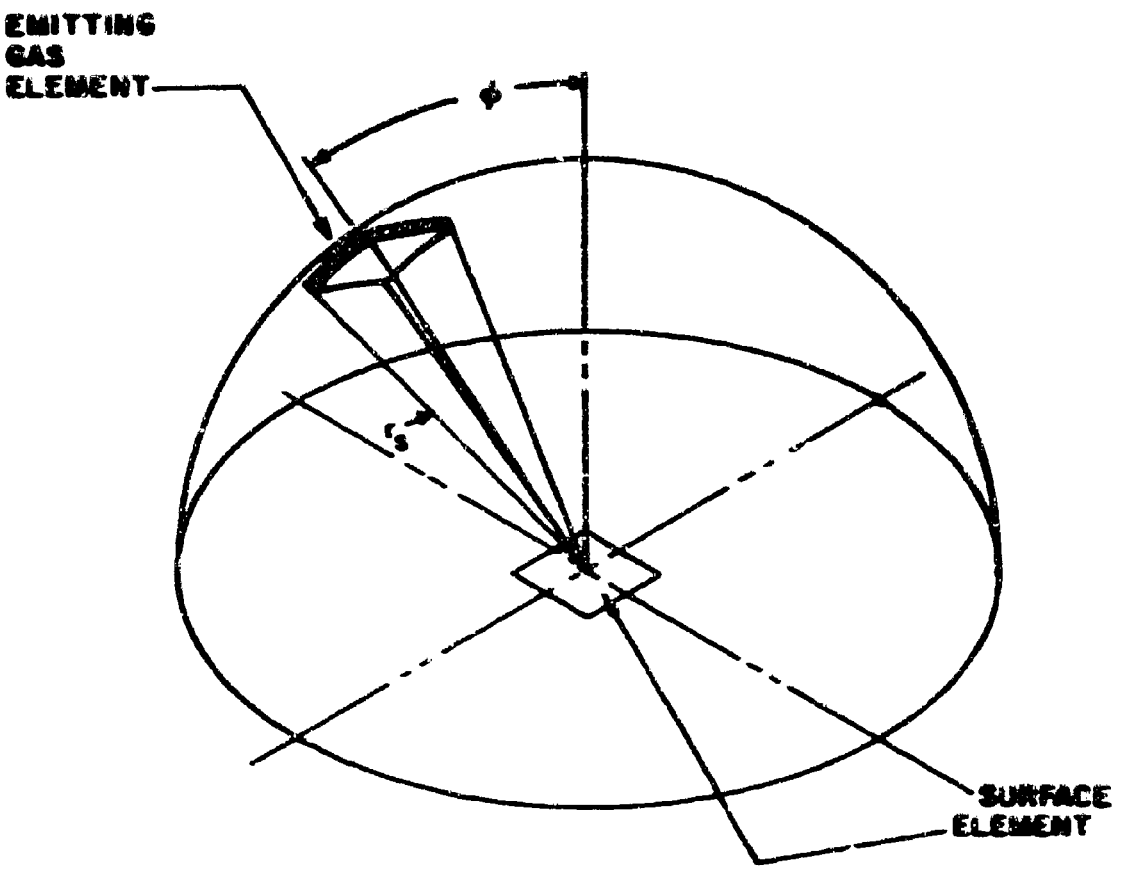

FIGURE 7 RADIATION EXCHANGE BETWEEN A HEMISPHERE OF GAS AND A SURFACE ELEMENT

volume of gas is:

$$4\,\sigma_{SB}\,T_G^4\,P_G\,\left(\frac{d\varepsilon_G}{d\,P_G\,\bar{\ell}}\right)\Big/_{P_G\bar{\ell}=0} \qquad (3\text{-}11)$$

The value of the differential of the gas emissivity is evaluated as if no radiation is absorbed by the intervening gases. The partial pressure of the absorbing gases present, P_G, accounts for this factor. Extension to the consideration of flame emission concerns the replacement of the gas values for those values found in the flame.

$$4\,\sigma_{SB}\,T_f^4\,P_G\,\left(\frac{d\varepsilon_f}{d\,P_G\,\bar{\ell}}\right)\Big/_{P_G\bar{\ell}=0} \qquad (3\text{-}12)$$

Inherent in this extension is the assumption that the flame consists of only carbon dioxide and water vapor. Such an assumption is valid for most combustion systems because CO_2 and H_2O are the only species present in large quantities which have sufficiently wide absorption bands to attenuate the radiation (McAdams, 1954). Thus the partial pressure is:

$$P_G = P_f\,(X_{CO_2} + X_{H_2O}) \qquad (3\text{-}13)$$

Hottel has also found that the value of the differential of ε_f is approximated by:

$$\left(\frac{d\,\varepsilon_f}{d\,P_G\,\bar{\ell}}\right)\Big/_{P_G\bar{\ell}=0} = \frac{3.6}{T_f} \qquad (3\text{-}14)$$

which may readily be utilized in the two dimensional formulation.

Using the equations developed above, the one dimensional analysis may be extended to consider two-dimensional exchange between all elements of the flame and an area of the wall (Anon., 1968). The total exchange is a function of the volume element of the flame, the emission per unit volume (Eqn. 3-12), the transmittance (a measure of radiation attenuation), and a view factor which will be described later. The problem considered and the symbols used are illustrated in Fig. 8.

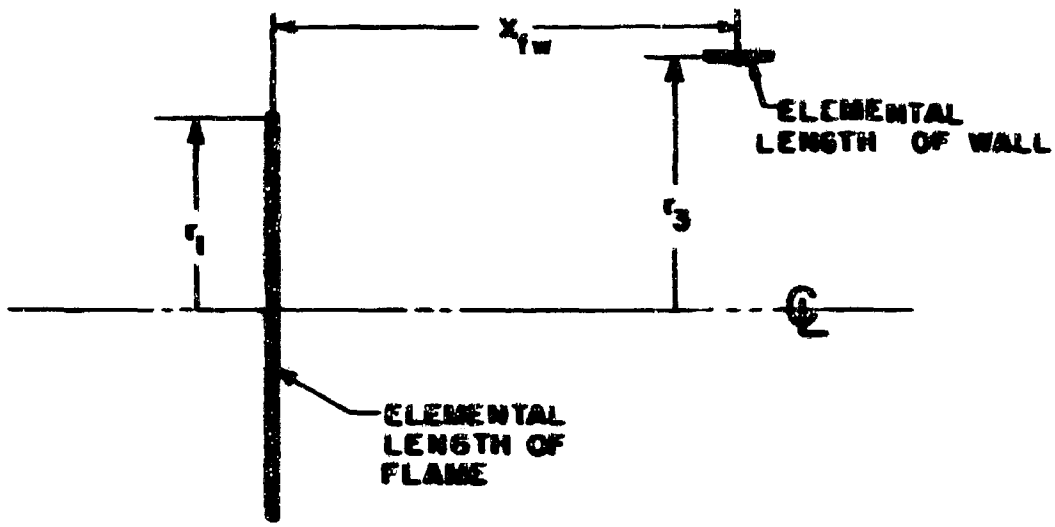

FIGURE 8 TWO DIMENSIONAL FLAME RADIATION

The elemental volume of the flame is considered to be the elemental length ΔX_f times the cross section of the combustion chamber at this point. Physically this seems to be a poor approximation, but under the assumption of one dimensional flow and a mean temperature across the chamber the analysis is as accurate as possible. Therefore, the volume of the flame element is:

$$\Delta X_f \cdot A_{X_{CS}} \tag{3-15}$$

where $A_{X_{CS}}$ denotes the cross section at that axial position.

The view factor, F_{fw}, may be defined as the radiant energy arriving at an element of the wall divided by the total energy leaving the flame element in all directions. The view factor is dependent on the specific geometry of the system and the determination is possible for most geometries of interest (McAdams, 1954, Sparrow and Cess, 1966). The determination of specific view factors may be found in numerous texts (McAdams, 1954, Sparrow and Cess, 1966, Howell and Siegel, 1969) and articles (Hamilton and Morgan, 1952) and further explanation or derivation would be necessary only if a specific geometry were being considered.

The transmittance is a measure of the energy emitted from the elemental flame volume which arrives at the wall element unattenuated. Attenuation is the result of absorption by the intervening gases. Hottel (McAdams, 1954) has provided typical empirical curves depending on the partial pressure of the gases present and the distance between the element of flame and the element on the wall, s. Northern Research (Anon., 1968) has correlated this result as shown in Fig. 9 using the following:

$$\Gamma = \frac{14.82}{P_G\, s + 14.82} \tag{3-16}$$

An average or mean value of the transmittance Γ_{mean}, has also been determined to account for the variation of s over the radius of the combustor for an annular combustor:

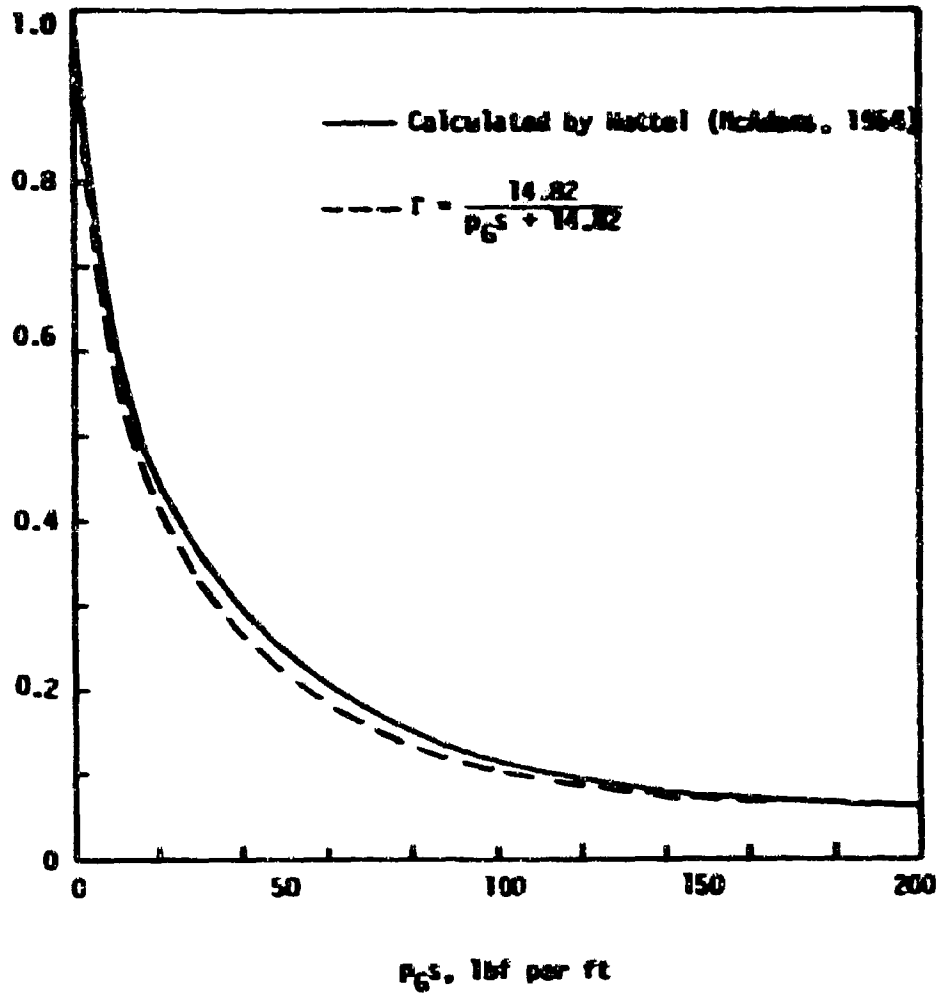

FIGURE 9 EFFECT OF PRESSURE AND GAS THICKNESS ON RADIATION TRANSMITTANCE (ABON., 1968)

$$\Gamma_{mean} = \frac{1}{n} \sum_{i=1}^{n} \frac{14.82}{14.82 + \Gamma_1} \qquad (3\text{-}17)$$

for which

$$\Gamma_1 = P_G \sqrt{X^2 + [r_3 - r_2 - (1/20 - 1/40)(r_1 - r_2)}$$

where n indicates the number of elements across the radius for which s was averaged.

Introducing the above variation into Eqn. (3-5) accounts for the emission of the flame element to the wall:

$$4\ \sigma_{SB}\ \Gamma_{mean}\ (\frac{1 + \alpha_w}{2}) P_G (\frac{d\varepsilon_f}{d\ P_G\ \ell})_0\ \Delta X_f\ A_{X_{CS}}\ F_{fw}\ (T_f^4 - T_w^4) \qquad (3\text{-}18)$$

The total radiant energy reaching the wall element will be the summation over all flame positions:

$$R_1 = \frac{4\ \sigma_{SB}\ (1 + \alpha_w)}{2} \sum_{\substack{\text{All Flame} \\ \text{Positions}}} [\Gamma_{mean}\ P_G\ (\frac{d\varepsilon_f}{d\ P_G\ \ell})_0 \cdot$$

$$\cdot\ \Delta X_f\ A_{X_{CS}}\ F_{fw}\ (T_f^4 - T_w^4)] \qquad (3\text{-}19)$$

The above formulation thus accounts for radiation reaching the wall element from all of the flame positions.

In conclusion, the methods of radiation transfer theory were not applied to the problem of flame radiation because of the mathematical complexity involved. Winter (1955) has provided a method to approximate the radiation exchange between an element of the flame and an element of the wall at the same axial location. Finally, the extension to determine the transfer from the entire flame to all axial positions was made using the analyses of Hottel (McAdams, 1954) and Northern Research and Engineering Corporation (Anon., 1968). Only one factor need be determined to calculate the radiation exchange using Eqn. (3-5), the flame emissivity. Determination of the emissivity of both luminous and nonluminous flames is the subject of the next section.

C. Flame Emissivity

The determination of flame emissivities has been an empirical matter in the majority of studies. The most widely used results are those of Hottel (McAdams, 1954) for carbon dioxide and water vapor, the assumption being that the flame consists mainly of these two emitters. This is true only for the case of nonluminous flames. Luminosity is the result of the presence of solid carbon particles emitting continuous radiation. The distinition between the two types of flames, the approximations made in the literature to calculate the emissivities of both categories from empirical results, and a brief review of theoretical approaches to the problem are discussed below.

The empirical charts prepared by Hottel (McAdams, 1954) are advantageous because they account for the emission of real gases (Einstein, 1963). Calculation of the emissivity from Hottel's results depends on the partial pressure of CO_2 and H_2O present in the flame, the characteristic radius of the geometry considered L, the flame temperature, and the wall temperature. The necessity of providing both the flame temperature and the wall temperature is based on Kirchoff's law (Winter, 1955); that is, the absorption of energy by the gas depends on the temperature of the emitter (in this case the wall at T_w) and emits energy at the temperature of the gas, T_G. Correction factors have been provided to account for changes in pressure and the variation in mole fractions of water and carbon dioxide present. One disadvantage of the results presented is that they are for one atmosphere and extreme extrapolation is required to obtain emissivities and absorptivities for typical gas turbine pressures (Anon., 1968). A second disadvantage is that for typical fuels and local fuel to air ratios, luminous carbon emission must somehow be added to the basic nonluminous radiation. To provide results for various partial pressures of CO_2 and H_2O and empirical results over a range of carbon particle concentrations would be a difficult task. For this reason, most investigations have chosen to use continuous functions to predict flame properties (Lefebvre and Herbert, 1960, Tipler, 1955, Anon., 1968, Aref and Sakkal, 1962, Thring et al., 1961, Beér and Claus, 1962).

A continous functional relationship has been found to correspond

to Hottel's charts within one or two per cent (Anon., 1968). For non-luminous flames the parameters on which the value of α_f and ε_f depend were included in relations suggested by Lefebvre and Herbert (1960):

$$\alpha_f \sim \phi_1 (r\bar{\ell})\ \phi_2 (P)\ \phi_3 (T_w) \qquad (3\text{-}20)$$

$$\varepsilon_f \sim \phi_1 (r\bar{\ell})\ \phi_2 (P)\ \phi_3 (T_f) \qquad (3\text{-}21)$$

Each of these factors were incorporated in the relation used by Lefebvre and Herbert (1960) which was provided by Reeves (Lefebvre and Herbert, 1960).

$$\varepsilon_f = 1 - \exp\left[1.60 \times 10^4\ P\ (r\ \bar{\ell})^{0.4}\ T_f^{-1.5}\right] \qquad (3\text{-}22)$$

For the remainder of the discussion the expression for absorptivity will be omitted; the only change necessary is to replace the flame temperature with the source temperature, T_w. However, Eqn. (3-22) only provides results for the nonluminous flame and not the luminous results which are of interest in some gas turbine studies.

The distinction between the emissions on a spectral basis of a luminous and nonluminous flame is illustrated in Fig. 10 and 11 from the work of Weeks and Saunders (1958). The emission rate variation over the spectrum substantiates the assumption made about the flame consisting primarily of H_2O and CO_2, excluding carbon monoxide. The emission bands of carbon dioxide are found at 1.9μ and 2.7μ. The 2.7μ band is overlaped with the H_2O emission band which has several peaks in the 2.7μ range. The presence of water is identified by the peak just below 2.6μ. If carbon monoxide were present in sufficient concentrations to attenuate radiation, there would be a peak in the 2.3 to 2.4μ range. Thus, it is concluded that for a typical fuel such as kerosene the omission of CO from consideration is acceptable.

Fig. 11 shows the spectral variation in emission rate due to the presence of carbon particles for a typical heavy composite fuel ("Mothball"). Two important factors are illustrated in this figure: firstly, radiation from the solid carbon particles is spectrally continuous rather

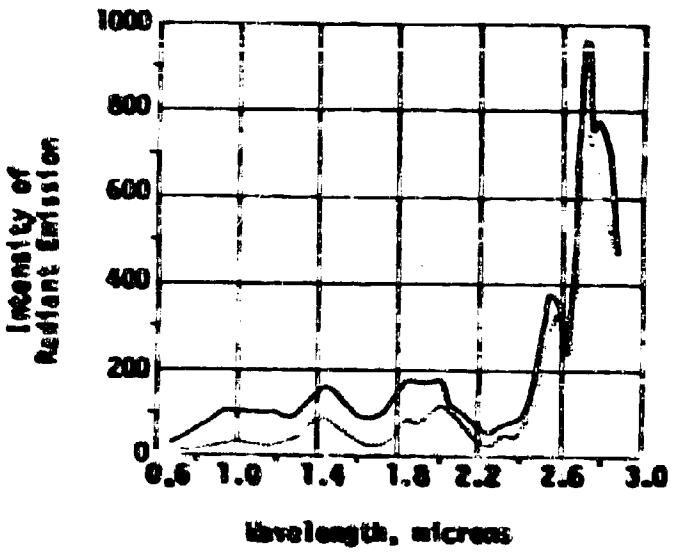

FIGURE 10 RADIATION FROM A NONLUMINOUS FLAME (WEEKS AND SAUNDERS, 1968)

____ 1-1/2 in. from burner

..... 11 in. from burner

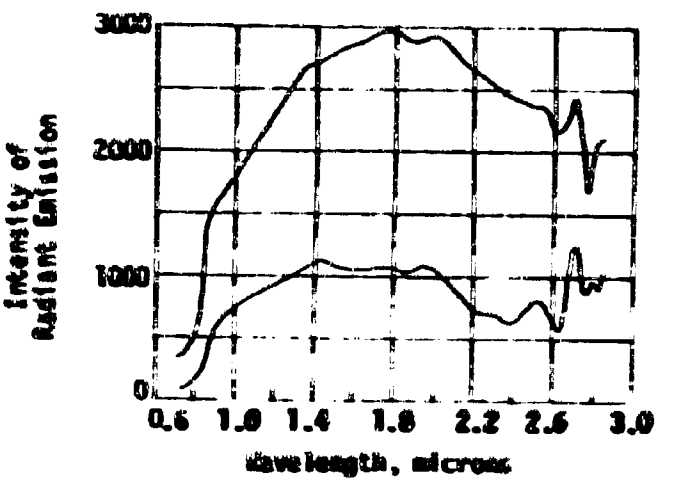

FIGURE 11 RADIATION FROM A LUMINOUS FLAME (WEEKS AND SAUNDERS, 1958)

Top curve 4 in. from burner

Bottom curve 13 in. from burner

than in discrete bands as found for gas emissions; secondly, the emission rate of carbon particles is considerably greater than that of the non-luminous H_2O and CO_2 radiation. The peak illustrated in Fig. 10 for CO_2 and H_2O in the 2.7μ range is seen on the right hand side of Fig. 11. The variation in magnitude is due to the higher heat release value of mothball fuel than for kerosene. In the discussion to follow, Fig. 11 illustrates why some authors have chosen to neglect the nonluminous radiation entirely.

Lefebvre and Herbert (1960) were the first to account for the variation in emissivity due to the luminous components with the addition of a constant factor to the emissivity equation, (Eqn. (3-22)).

$$\varepsilon_f = 1 - \exp\left[1.6 \times 10^4 \, \Lambda \, P(r\bar{\ell})^{0.5} \, T_f^{-1.5}\right] \qquad (3\text{-}23)$$

The factor Λ is strictly an empirically determined factor. Typical values for various fuels are shown in Table 2 (Lefebvre and Herbert, 1960). Note the difference in the luminous factor for the two fuels, kerosene and mothball, shown in Figs. 10 and 11. Lefebvre and Herbert determined that the luminosity factor Λ could be correlated to the carbon to hydrogen ratio of the fuel in use by the following:

$$\Lambda = 7.53 \, (C/H - 5.5)^{0.84} \qquad (3\text{-}24)$$

Northern Research (Anon., 1968) has attempted to correlate the luminosity factor to provide results more accurate than Lefebvre and Herbert's. Firstly, an exponential relation of the form:

$$\Lambda = \exp\left(\frac{C/H - 4.4}{2.3}\right) \qquad (3\text{-}25)$$

was tried and the results are shown in Fig. 12 compared to the data of Schirmer and Quigg (Anon., 1968). A recorrelation of the results has been provided of the form:

$$\varepsilon_f = 1 - \exp\left[4.7 \, p^{1.3} \, \Lambda \, (r\bar{\ell})^{0.5} \, T_f^{-1.5}\right] \qquad (3\text{-}26)$$

Table 2.

Luminosity Factors for Various Fuels
(Lefebvre and Herbert, 1960)

Fuel	Λ
Kerosene	1.7
Gas Oil	6.7
Mothball	16.2
Tarmac	19.1

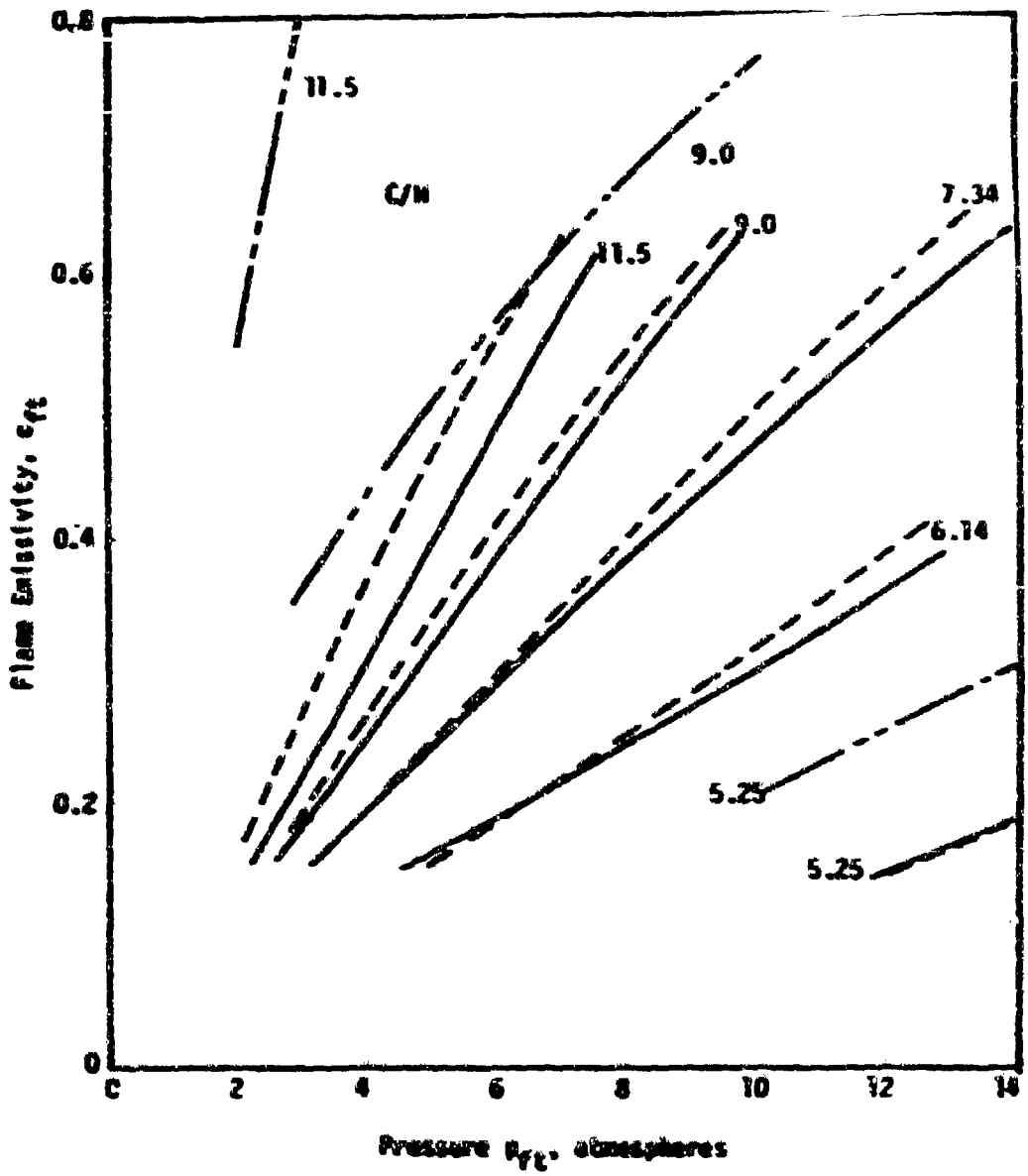

FIGURE 12 FLAME EMISSIVITY CORRELATION COMPARISON WITH EXPERIMENTAL DATA (ANON., 1968)

_____ Data from Schirmer and Quigg (Anon., 1968) assuming T_{ft} = 3500 deg K

_ _ _ Values predicted from IHEC 1966 correlation (Eqn. 3-26)

_ _ _ _ Values predicted from IHEC 1964 correlation (Eqn. 3-25)

where

$$\Lambda = \left(\frac{C/H - 5}{0.16}\right)^{0.74}$$

The results for the revised correlation which uses a luminosity factor similar to the Lefebvre correlation with a power law dependence on pressure in the exponential term are also presented Fig. 12.

In an attempt to provide a physical basis for the luminosity factor, Hottel (McAdams, 1954), Thring et al. (1962), and Beér and Claus (1962), have suggested expressions of the form:

$$\varepsilon_f = 1 - \exp\left[-C \ell f(\lambda)\right] \qquad (3\text{-}27)$$

where C is the soot or carbon particle concentration, ℓ the mean free path, and $f(\lambda)$ is a function of the wavelength, particle size, and particle distribution. Thring et al. (1962) assumed that the luminous flame behaved similarly to a turbid medium. By application of light scattering theories, the authors claim to have derived the following relation:

$$\varepsilon_f = 1 - \exp\left[-K_1 \bar{C} \bar{\ell}\right] (1 - \varepsilon_\eta) \qquad (3\text{-}28)$$

where $\bar{C}$ is the average soot concentration. This is in contrast to the formulation found from empirical results:

$$\varepsilon_f = 1 - \exp\left[-K_1 C_{max} \bar{\ell}\right] (1 - \varepsilon_\eta) \qquad (3\text{-}29)$$

where C_{max} is the maximum soot concentration and ε_η accounts for the nonluminous radiation factor. Thring et al. assumed the particles were in one of two classes: spherical units of from 100 to 800 Å with a nominal size of 400 Å or spheres from 1 to 15μ.

Stull and Plass (1960) investigated the interaction of electromagnetic waves with particles ranging from 50 to 1000 Å, developing the optical theories by considering the particles to be equally dispersed. The restricting assumptions made by Sato et al. (1962) are typical of th s

type of investigation. The particles were assumed to be identical in size and material and to be equally dispersed throughout the flame. The temperature of the cloud was also assumed to be uniform. The physical insight gained by investigating such a system rather than assuming a constant factor of luminosity is lost in the idealities of the model proposed. This criticism is specifically pointed to the assumption of a uniform dispersion and temperature in the flame.

In conclusion, with the present knowledge concerning carbon formation in flames, the assumptions necessary to arrive at an entirely analytical solution have little practical applicability. The accuracy and convenience of the continuous function appear to have overshadowed the empirical charts of Hottel, especially with the addition of luminous radiation. However, the expressions used must be verified as to the accuracy attainable when extrapolated to higher pressures.

D. Radiation Exchange Between the Chamber Walls

The consideration of radiation exchange between different areas of the wall was originated in the work of Tipler (1955). The specific case considered was the exchange between the wall in the primary zone and that of the secondary zone. A similar analysis was derived to determine the general exchange between wall areas for an annular combustor (Anon., 1968).

The analysis as proposed by Tipler suggests that the exchange between the primary wall of a tubular combustor and the secondary wall should be given by an equation similar to Eqn. (3-5):

$$\Delta R_3 \sim \sigma_{SB} F_{dA_1-dA_2} [\varepsilon_w T_{w_1}^4 - \alpha_w T_{w_2}^4] \qquad (3\text{-}30)$$

where α_w and ε_w will be approximatly the same and the view factor, $F_{dA_1-dA_2}$ will depend on the geometry and type of the combustor. Appropriate view factors are found in numerous heat transfer texts (Sparrow and Cess, 1966, McAdams, 1954). Tipler included an additional factor, $(1 + \varepsilon_f)$, which accounts for the absorption by the flame. The situation considered is illustrated in Fig. 13 and follows the relation:

$$\Delta R_3 = (1 - \varepsilon_f) F_{dA_1-dA_2} \sigma_{SB} [\varepsilon_w T_{w_1}^4 - \alpha_w T_{w_2}^4] \qquad (3\text{-}31)$$

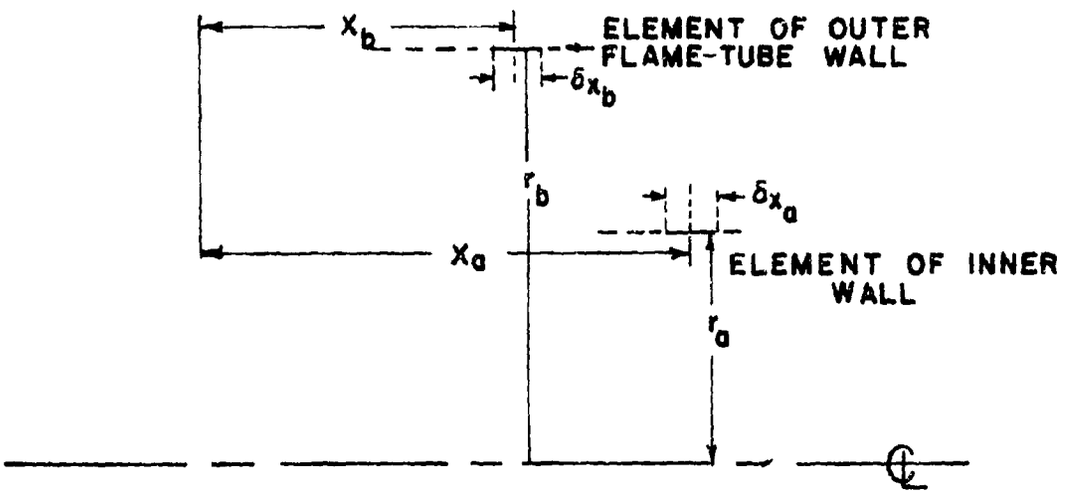

FIGURE 13 RADIATION INTERCHANGE BETWEEN FLAME-TUBE WALLS

Since $\alpha_w = \varepsilon_w$ for most conditions:

$$\Delta R_3 = (1 - \varepsilon_f)\, \varepsilon_w\, \sigma_{SB}\, F_{dA_1\text{-}dA_2} [T_{w_1}^4 - T_{w_2}^4] \qquad (3\text{-}32)$$

Northern Research (Anon., 1968) has provided a similar analysis which, rather than accounting for a flame, accounts for the absorption of the intervening gas between the two areas. Under the assumption that the flame consists of CO_2 and H_2O the two analyses are conceptually the same. The transmittance of radiation, Γ, is determined with Eqn. (3-16).

$$\Delta R_3 = \sigma_{SB}\, \varepsilon_w\, F_{dA_1\text{-}dA_2}\, \Gamma\, (T_{w_1}^4 - T_{w_2}^4) \qquad (3\text{-}33)$$

Summation over all wall positions yields:

$$R_3 = \sigma_{SB}\, \varepsilon_w \sum_{\substack{\text{All Wall} \\ \text{Positions}}} F_{dA_1\text{-}dA_2}\, \Gamma\, (T_{w_1}^4 - T_{w_2}^4) \qquad (3\text{-}34)$$

Similar expressions represent the exchange between each of the wall elements and the remainder of the system.

E. Radiation Exchange Between the Chamber Wall and the Casing

With the basic principles of radiation exchange having been presented, the presentation of the methods used to determine R_2 is relatively brief. The only variation found in the formulation is the replacement of the wall temperature in Eqn. (3-30) with the casing temperature T_{CA} (Anon., 1968, Lefebvre and Herbert, 1960).

$$R_2 = F_{W\text{-}C}\, \sigma_{SB}\, (T_w^4 - T_{CA}^4) \qquad (3\text{-}35)$$

Two assumptions are not immediatly evident in Eqn. (3-35). First, the view factor must account for direct exchange and exchange through reflection and rereflection. A typical expression has been given by Northern Research (Anon., 1968) as:

$$\frac{1}{F_{WC}} = \left(\frac{1}{\varepsilon_w} - 1\right) + \frac{A_w}{A_{CA}} \left(\frac{1}{\varepsilon_{CA}} - 1\right) + \frac{1}{F_{WC}} \qquad (3\text{-}36)$$

where:

$\overline{F_{wc}}$ ≡ black-surface overall view factor

A_w ≡ area of the wall

A_{CA} ≡ area of the casing

ε_{CA} ≡ emissivity of the casing ($\varepsilon_{CA} = \alpha_{CA}$)

Second, the gases present in the annulus do not attenuate radiation. This corresponds to the fact that O_2 and N_2 do not absorb or emit radiation in the infrared (McAdams, 1954). The summation necessary for the chamber wall interchange is not necessary because the casing is assumed to have a constant temperature (Anon., 1968). The variation due to combustor geometry affects only the exchange factor.

CHAPTER IV

CONVECTIVE HEAT TRANSFER IN COMBUSTION CHAMBERS

A. Introduction

The evaluation of the heat transfer terms C_1 and C_2 has received considerably less attention than the problem of radiation in the combustion chamber. Methods for calculating the internal convection near the front of the chamber have been presented in the literature, but the impression left is that the particular investigators realized convective heating occurred and thus a term accounting for it was necessary. The problem centers around the diversity of recirculation flows found in the region and the prediction of their magnitude and direction. In sharp contrast is the vast number of studies concerning film cooling, a variation of internal convection. Unfortunatly most studies have been performed with either low mainstream temperatures, on the order of 100 to 200°C, or with heated slot flow and cold mainstreams. The use of these correlations to predict extrapolated conditions could be extremely misleading. Spalding (1965) has provided a semi-empirical theory which indicates the correct trends and provides a basis of comparison with experimental results. The final source of internal convection, the penetration jet, has not been considered at all in any of the heat transfer analyses found, for reasons which will be discussed later. The first portion of this chapter concerns the review of the literature written before 1966 regarding these internal modes of convection.

External to the flame tube, the convective cooling C_2 is a much easier mode to analyze. The reduction in flow velocities are relatively easy to determine and the cooling is not dissimilar to flow over a flat plate. The difference in the difficulty in determining internal and external convective contributions is the difference found in modelling the flow conditions in the two regions. The final topic to be covered

is thus the analysis of the convection due to external flow, C_2.

B. Internal Convection, C_1

B. 1) Convective Heating in the Absence of Secondary Flow

In the front portion of the primary zone is a region in which little secondary air has been added through penetration jets or film cooling slots. The gases present have either entered through holes in the dome or have recirculated in a manner similar to that shown in Fig. 2. The difficulties encountered in modelling this flow have been discussed previously (Hammond and Mellor, 1971). Of the analyses concerning heat transfer in combustion chambers (Lefebvre and Herbert, 1960, Tipler, 1955, Winter, 1955), only Lefebvre and Herbert have even considered the effects of flow in this region. Due to the stratified flow in the primary zone and the fact that gases are undergoing rapid physical changes in this region, the authors admitted that an account of the convection would at best be highly approximate. The analogy proposed is to model the flow as straight pipe flow. The expression for such a flow is:

$$St = 0.0283\ Re^{-0.2} = 0.0283\ \left(\frac{Q_p}{A_p}\frac{d_p^*}{\mu}\right)^{-0.2} \qquad (4\text{-}1)$$

or

$$C_1 = 0.020\ \frac{\alpha}{\mu}\,0.8\ \left(\frac{Q_p}{A_p}\right)^{0.8}\ \frac{(T_G - T_w)}{d_p^{*\,0.2}} \qquad (4\text{-}2)$$

where Q_p is the mass flow rate, A_p the cross sectional area, and d_p^* the hydraulic diameter, all of the primary zone. Immediately upon statement of the above formulation Lefebvre and Herbert express some doubt as to the validity of the equation. Firstly, the flow velocity near the wall is found to be higher than the mean velocity in the primary zone because of the necessity of such a flow to stabilize the flame. Secondly, the use of swirl further increases the approximate nature of the solution. Finally, the temperature of the gases near the wall is lower which will lead to higher gas densities near the wall and further exaggerate the velocity effects mentioned before.

An additional problem is found in determining the temperature at

which the properties of the fluid should be analyzed. For radiation, the bulk gas temperature may be satisfactory, but due to the stratification of temperature in the flow, the value of T_c for convection will be somewhere between T_f and T_w.

Calculation of the convective heating in the above manner after secondary air has been added will become a progressively better approximation at positions down the chamber since the recirculation flow will disappear and the flow become more analogous to pipe flow.

In conclusion, the determination of C_1 in the primary zone has received very little attention in the literature. The flow has been modelled as being similar to pipe flow. The error involved in such an analogy will depend on how closely pipe flow resembles the true situation in the combustor geometry considered. Fortunately, a large portion of the secondary zone region is cooled by film and splash cooling devices for which the cooling effects are better understood.

B. 2) Film Cooling of Chamber Walls

To protect the chamber wall from convective heating, design practices have dictated the use of film cooling slots. The film cooling slot (Fig. 14) provides a blanket of cool annulus air to protect the liner wall from the hot chamber gas. The cooling flow may consist of three distinct zones: the potential core, the wall jet region, and the fully developed turbulent boundary layer region. The character and the existence of these regions depends on the ratio of coolant or slot gas velocity, u_s, to the magnitude of the free stream velocity, u_{ms}. For slot velocities much greater than the mainstream velocity, $u_s >> u_{ms}$, the wall jet velocity may be calculated utilizing Glauert's (1956) wall jet theory. For the case where $u_{ms} >> u_s$ the wall jet region no longer exists (Stollery and El-Ehwany, 1965). The flow transition is thus from the potential core flow directly to the fully developed turbulent boundary layer flow. Because both of the situations are found in combustion chambers, the theories and experimental evidence pertaining to each will be reviewed.

Of the numerous works related to film cooling, the majority concern

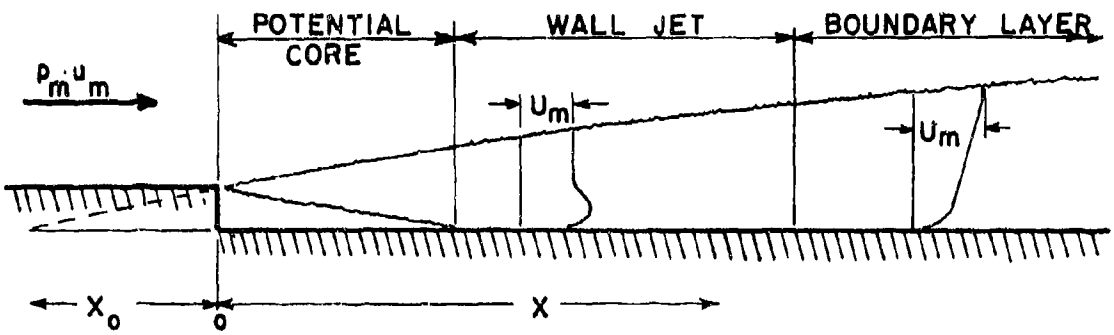

FIGURE 14 FILM COOLING SLOT AND FLOW REGIONS

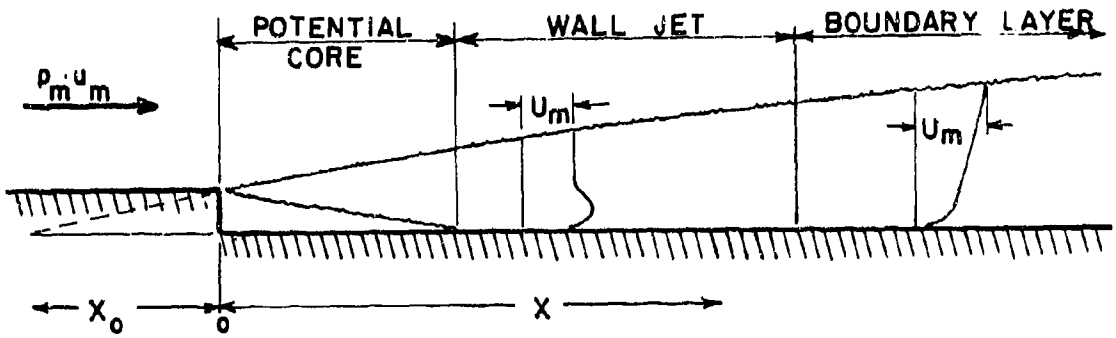

FIGURE 14 FILM COOLING SLOT AND FLOW REGIONS

the turbulent boundary layer region; considerably less work has been done on the wall jet flow and almost none on the potential core. In the case of the wall jet, the theory of Glauert (1956) will be reviewed and the success of the theory compared to the experimental findings of Seban and Back (1960). Spalding (1965) has proposed a semi-empirical theory which encompasses both the wall jet and turbulent boundary layer region. The basis for the theory will be reviewed and the wall jet solution contrasted to that of Glauert. The solution for the turbulent boundary layer will be stated as a guide to presenting the numerous experimental investigations of the turbulent region. Hopefully, the order chosen for the review will provide substantially greater insight into the numerous correlations presented in the literature.

Throughout the literature, the investigations (both theoretical and experimental) employ the "adiabatic wall" for their studies. This is merely a reference state which avoids the introduction of extraneous phenomena into the results. Without such a reference state, the results of the various authors could not accurately be compared. Additionally, the scatter found in the results of the various investigators may be partially attributed to insufficiently adiabatic walls.

B. 2-1) The Potential Core Region

The potential core exists from the slot exit until the turbulence induced by the mainstream mixes the slot and mainstream flows (see Fig. 14). The gases below the mixing line retain the properties of the coolant flow. For this reason, in the absence of radiative heating, the adiabatic wall temperature will be that of the coolant flow (the effect of radiative transport is included through the use of the theory of superpositing as described in Chapter III). Thus, the convective heat transfer is determined using Newton's convective heat transfer equation (McAdams, 1954):

$$q_c = h_c A (T_w - T_s) \qquad (4\text{-}3)$$

where the value of h_c, the convective heat transfer coefficient, is that of laminar flow over a flat plate, T_w is the adiabatic wall temperature, and T_s the temperature of the slot fluid. Assuming the region behind

the slot is similar to a flat plate is acceptable because the normal slot height is sufficiently small, compared to the radius of the chamber, that effects due to the curvature will be negligible. An additional assumption is that the slot is continuous around the chamber to avoid the inclusion of end effects. In conclusion, the potential core in the absense of radiation is unaffected by the presence of the mainstream thus protecting the wall from convective heating.

B. 2-2) The Wall Jet Region

The wall jet flow region velocity profile (Fig. 14) indicates why the wall jet must be considered as a specific type of flow rather than as a fully developed turbulent boundary layer. The flow near the wall is characteristic of the viscous effects of the boundary layer. The unique property of the flow is the peaked velocity profile near the wall which slowly dissipates to the freestream value as the end of the velocity boundary layer is approached. Of course, such a region does not exist when the coolant flow velocity is less than or of the order of the magnitude of the mainstream velocity.

The pioneering study of the wall jet was conducted by Glauert (1956), who solved the boundary layer problem for the velocity profile assuming there is a similarity solution such that the velocity $u \sim x^a$ and the velocity boundary layer thickness δ is proportional to x^b, $\delta \sim x^b$. The value of a and b must be found. The equations of interest for the system are the two dimensional continuity equation:

$$\frac{\partial \bar{u}}{\partial x} + \frac{\partial \bar{v}}{\partial y} = 0 \qquad (4\text{-}4)$$

and the momentum equation:

$$\bar{u} \frac{\partial \bar{u}}{\partial x} + \bar{v} \frac{\partial \bar{u}}{\partial y} = \frac{\partial}{\partial y} \left(\epsilon_\tau \frac{\partial \bar{u}}{\partial y} \right) \qquad (4\text{-}5)$$

where the bars above the velocity components represent the mean velocity of the flow. It should be noted that the eddy viscosity has been used in place of the two terms for viscosity in Eqn. (2-2). The boundary conditions available for Eqn. (4-4) and (4-5) are:

$$\bar{u} = \bar{v} = 0 \text{ at } y = 0 \text{ and } \bar{u} \to u_{ms} \text{ as } y \to \infty \qquad (4\text{-}6)$$

For the use of Glauert's formulation it will be required that the mainstream velocity approach zero.

To simplify the task, Glauert used Prandtl's hypothesis to describe the behavior of ε_T, that the eddy viscosity is constant across the boundary layer and proportional to the product of the maximum mean velocity, $\bar{u}_{max}$ and δ, the boundary layer thickness.

Assuming there is a similarity solution for the velocity profile and that $\bar{u} \sim x^a$ and $\delta \sim x^b$, Glauert determined that $\varepsilon \sim x^{a+b}$, where $b = 1$ and $a = -4/3$. By defining stream functions and integrating to solve Eqn. (4-5) Glauert found his results gave the characteristic results of the outer portion of the laminar wall jet shown in Fig. 15. To account for the remainder of the flow, Glauert incorporated the frictional effects found in turbulent pipe flow studies by Blasius:

$$\tau = 0.0225\, \rho\, \bar{u}^2 \left(\frac{\mu}{\bar{u}y}\right)^{1/4} \qquad (4\text{-}7)$$

that is, the frictional effect of the wall has been accounted for as a function of the parameters of the system. The result of matching the theoretical profile provided by Prandtl's hypothesis for the flow beyond the maximum velocity with the empirical results of Blasius is shown in Fig. 16, where η_δ and f' are the nondimensional distance and velocity functions.

Glauert also defined a function, α_{WJ}, which is a measure of the extent of the frictional effects on the flow for the velocity profile beyond the maximum velocity. This function will be of use later in studying the empirical results of Seban and Back (1960).

The above is a cursory review of the work of Glauert and in no way implies the solution for the boundary layer is a simple one. However, the analytical aspects have been avoided because the experimental results will provide needed information. The temperature profiles cannot be obtained from Glauert's numerical solution by a technique such as the application of Reynold's analogy (Schlichting, 1960) because the

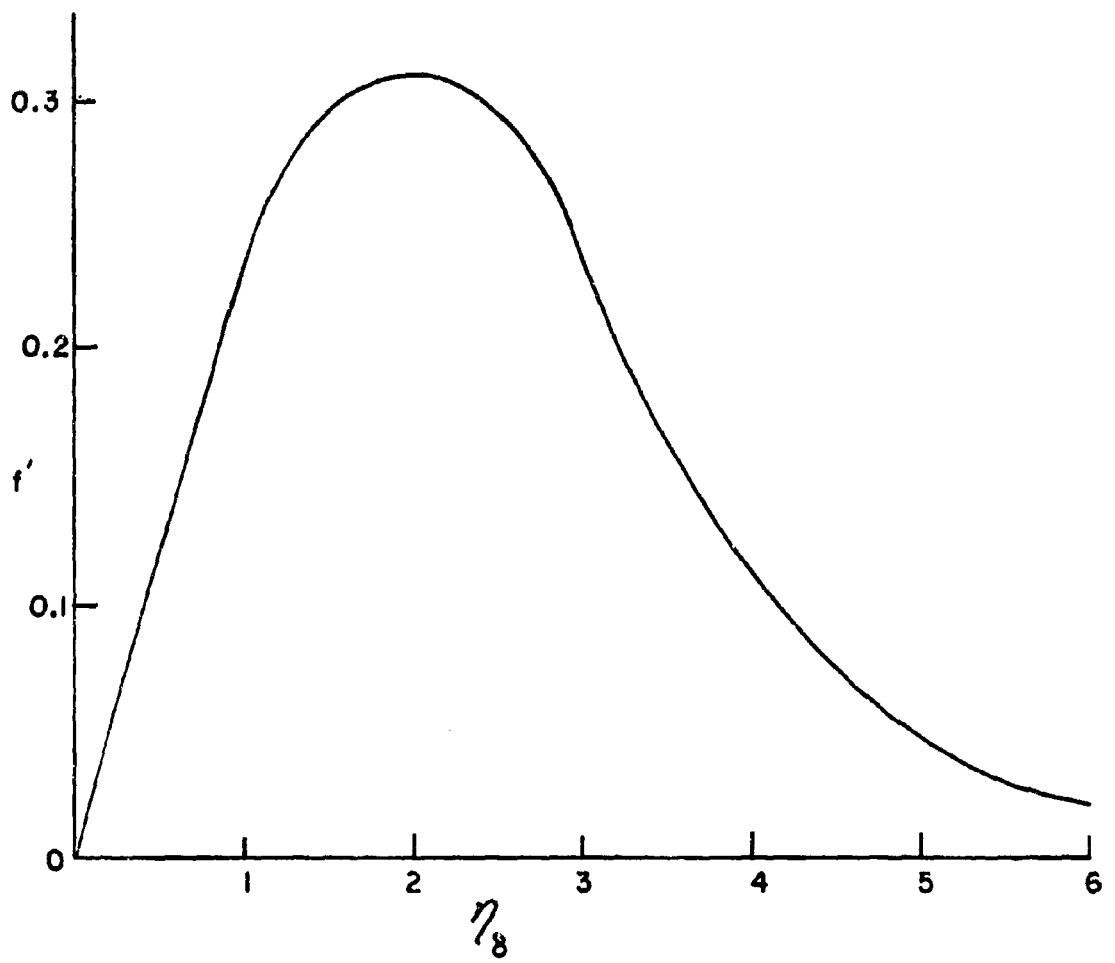

FIGURE 15 VARIATIONS OF VELOCITY (f') WITH DISTANCE FROM THE WALL (η) FOR A LAMINAR WALL JET (GLAUERT, 1956)

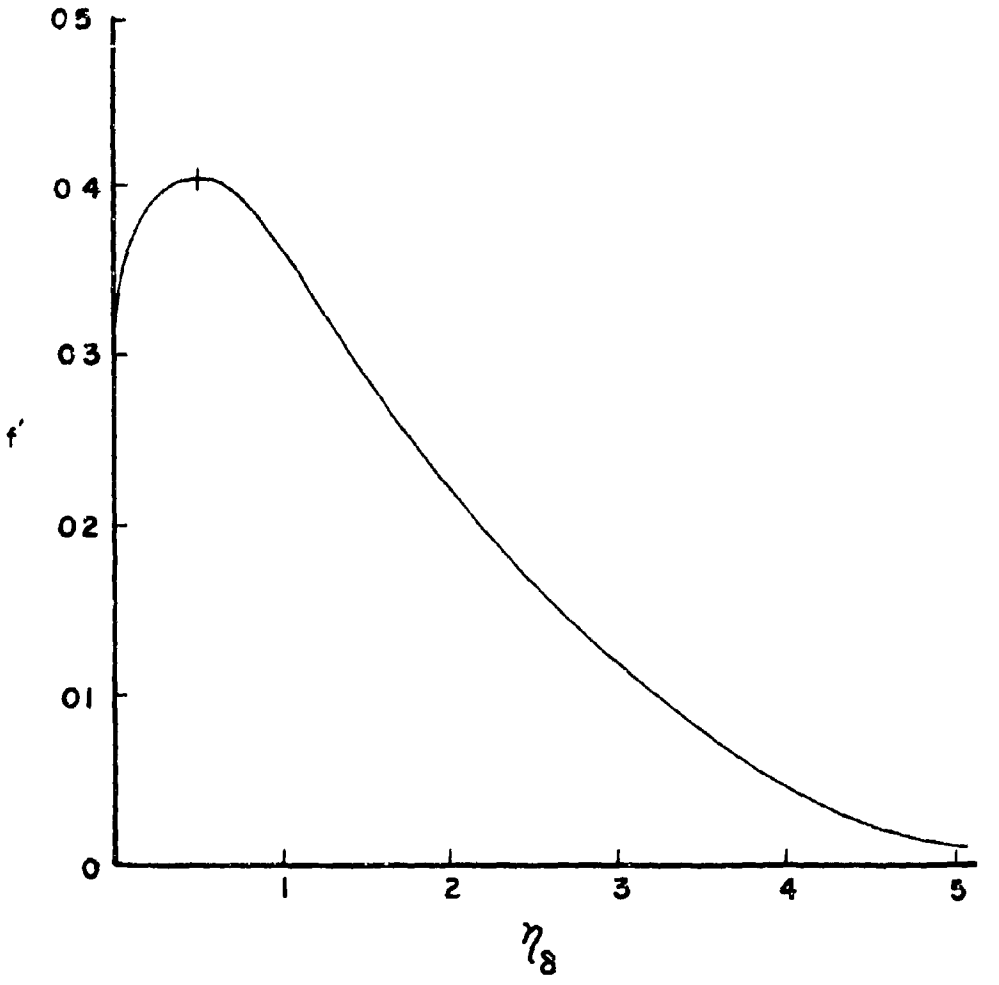

FIGURE 16 GLAUERT'S (1956) RESULTS FOR THE TURBULENT WALL JET VELOCITY PROFILE

flow and temperature fields are not analogous. Therefore, Seban and Back's (1960) results have to be used rather than extending Glauert's theory to temperature profiles.

These investigators empirically determined the velocity and temperature profiles in the wall jet. The analysis used strictly follows the work of Glauert reviewed above. The system Seban and Back studied is depicted in Fig. 17. The authors indicated that the difficulty in applying Glauert's results stems from the velocity expression:

$$u = U\left[\frac{4 - 4b}{\lambda_{WJ}}\left(\frac{Ux}{\mu}\right)^{4-5b}\frac{df}{d\eta_\delta}\right] \tag{4-8}$$

where U is a reference velocity which is not easily defined, λ_{WJ} a function which depends on the ratio of the nondimensional distance from the wall to the maximum velocity, to the nondimensional distance from the maximum velocity to the end of the boundary layer. The proportionality is defined by α_{WJ} which in turn yields the power of $\bar{u} \sim x^a$ and $\delta \sim x^b$ by:

$$a = -\frac{4\alpha_{WJ}}{5 + \alpha_{WJ}} \tag{4-9}$$

$$b = \frac{4 + 4\alpha_{WJ}}{5 + 4\alpha_{WJ}} \tag{4-10}$$

or approximately:

$$a = -\frac{\alpha_{WJ}}{1 + \alpha_{WJ}} \tag{4-11}$$

$$b = 1 \tag{4-12}$$

The function $df/d\eta_\delta$ is related to the similarity variable η_δ which is given by:

$$\eta_\delta = \frac{4 - 4b}{\lambda_{WJ}}\frac{yU}{\mu}\left(\frac{Ux}{\mu}\right)^{-b} \tag{4-13}$$

In actuality, the coordinate $f' = df/d\eta_\delta$ of Fig. 16 is nondimensionalized as follows:

$$\frac{df}{d\eta_\delta} \Big/ \left(\frac{df}{d\eta_\delta}\right)_{max}$$

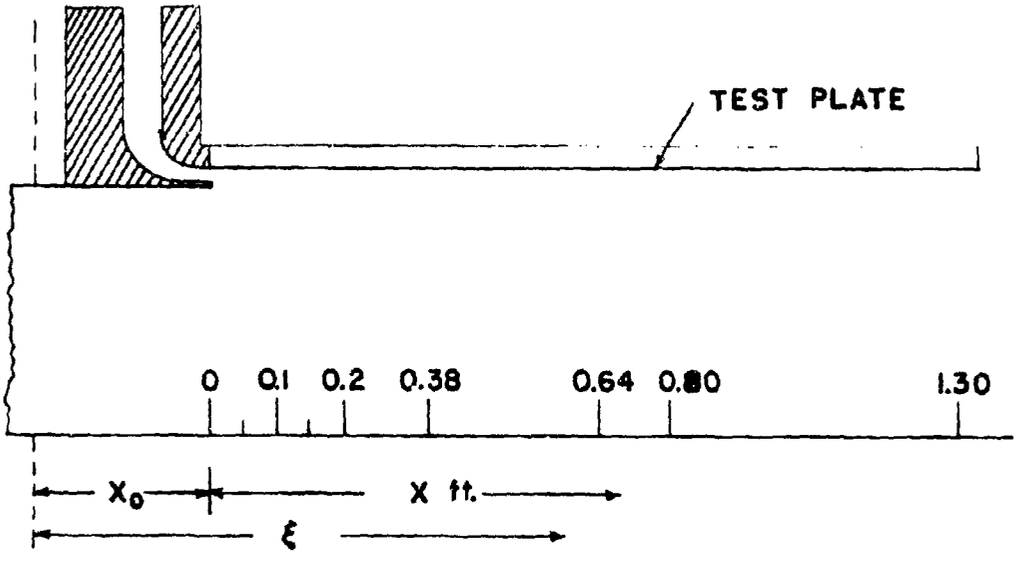

FIGURE 17 EXPERIMENTAL SYSTEM OF SEBAN AND BACK (1960)

$$\frac{2\eta_\delta}{(\eta_\delta)_{max}\,\delta} = \frac{2y}{\delta} \qquad (4\text{-}14)$$

with $\delta/2$ being the distance from the wall to where $\bar{u} = 1/2\ \bar{u}_{ms}$. A value of $\delta/2$ is used for the related variable because this is the easiest experimental point to determine with sufficient accuracy.

Fig. 16 compares extremely well with the results of Seban and Back. Generally, it was found that as the slot height was reduced the agreement with the theoretical results improved. This does not imply that the results were drastically far from the theoretical predictions at large slot heights, becuase the accuracy was still fairly good. Of interest to the application of modelling film cooling flow was the fact that the influence of the free stream flow was noted even for mainstream velocity ratios $\bar{u}_m/\bar{u}_{max}$ of 0.40.

Seban and Back have correlated their data in terms of ξ, which is the distance downstream of the slot, x, plus the starting or effective starting length of the boundary layer, x_o:

$$\xi = x + x_o \qquad (4\text{-}15)$$

From Glauert's results the following analytical function was compared with the empirical results:

$$\frac{\xi}{h'_s} = \frac{x_o}{h'_s} + \frac{x}{h'_s} = \left(\frac{\delta}{h'_s}\right)\left(\frac{\delta\,\bar{u}_{max}}{\mu}\right)^{1/4} x \cdot \cdot \left[\frac{4}{0.0275}\left(1 - \frac{4 + \alpha_{WJ}}{5 + \alpha_{WJ}}\right)(\alpha_{WJ} + 0.07)\,\eta_\delta^{-5.4} \cdot \cdot \left(\frac{f_{max}}{f'_{max}}\right)^{5/4}\right] \qquad (4\text{-}16)$$

for which f_{max}, f'_{max} and η_δ are functions of α_{WJ}. Experimental results indicate that the power law behavior may not exist far downstream of the slot. This region is of no importance for practical film cooling results and will not be discussed.

For the experimental values, it was found that:

$$\frac{\bar{u}_{max}}{u_s}\frac{\delta}{n_s} = 0.212\left(\frac{\xi}{n_s}\right)^{0.60} \qquad (4\text{-}17)$$

which agrees with experimental results within 5 per cent. Similarly,

$$\frac{\bar{u}_{max}}{u_s} = 3.6\left(\frac{\xi}{h_s}\right)^{-0.45} \qquad (4\text{-}18)$$

for all slots within a 5 per cent error.

Seban and Back extended Glauert's work by analytically determining the expected shape of the temperature profiles. The result is compared with the experimental profiles in Fig. 18 for a 0.25 inch slot. The profiles near the slot approach a zero slope near the wall as would be expected.

D. B. Spalding (1965) developed a theory which includes all possible interactions of film cooling slots with a flat plate. In actuality, the theory was developed to include mass transfer through a flat plate and combustion in the boundary layer, as well as film cooling flow. Because of its substantial length, the theory will only be briefly outlined: the results for the wall jet will be presented as the final part of this section and the results for the turbulent boundary layer will lead into the subsequent discussion of film cooling.

The "Unified Theory" of Spalding was an attempt to organize the extensive experimental work done on film cooling (Chin et al., 1958, Chin et al., 1961, Hartnett et al., 1961, Hatch and Papell, 1961, Papell, 1960, Papell and Trout, 1959, Seban, 1960, Seban and Back, 1962, Back and Seban, 1962, Seban et al., 1957, Seban and Back, 1960, Stollery and El-Ehwany, 1965). Each of these investigators have varied the mainstream velocity or temperature, the coolant flow and temperature, correlated the results, and presented this correlation usually with use of very little physical insight. A second difficulty with the experimental results is that the conditions under which the film cooling was studied were usually at low mainstream temperatures (less than 700°R) or with a cold mainstream and heated slot flow. Therefore, the correlations determined cannot be reliably extended to the range of interest in combustors.

Fig. 19 is a graphical representation of the possible situations

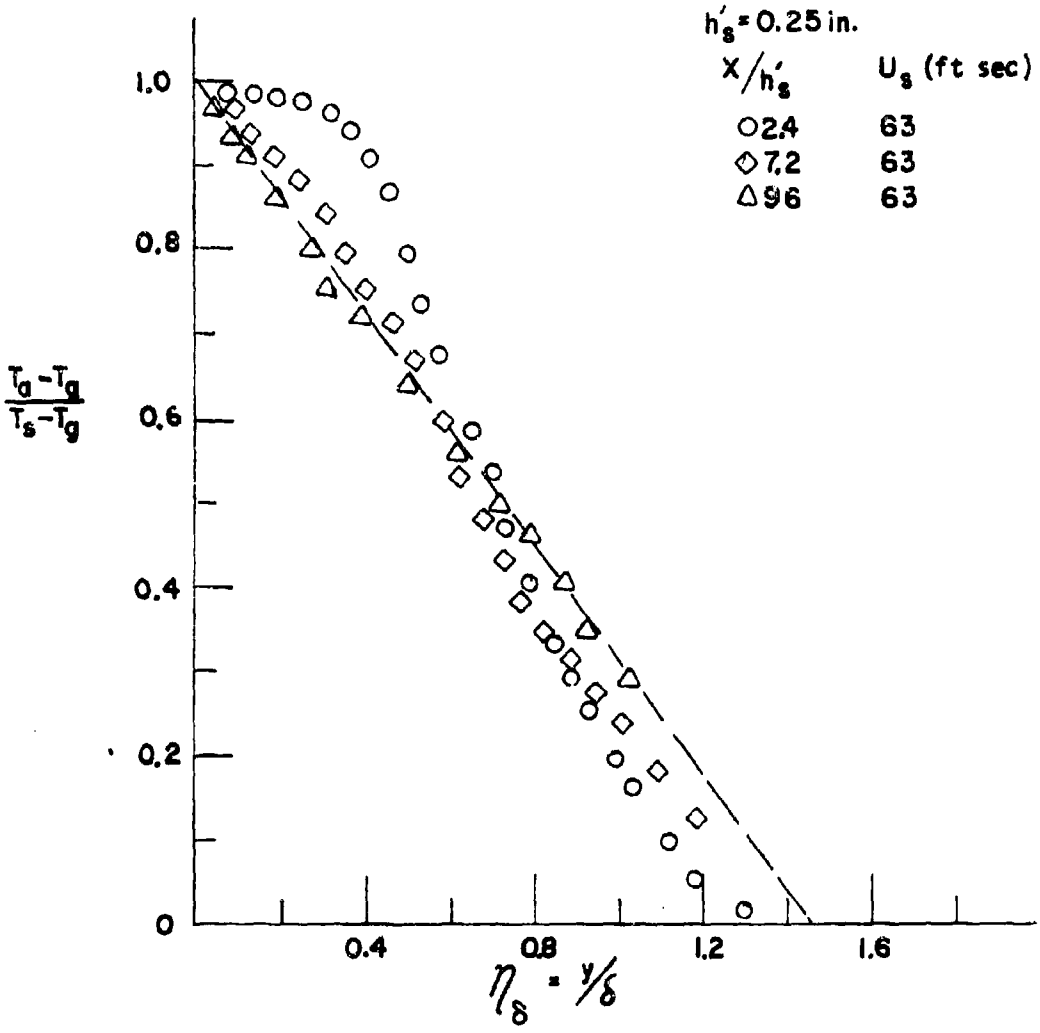

FIGURE 18 EXPERIMENTAL RESULTS OF SEBAN AND BACK (1960)

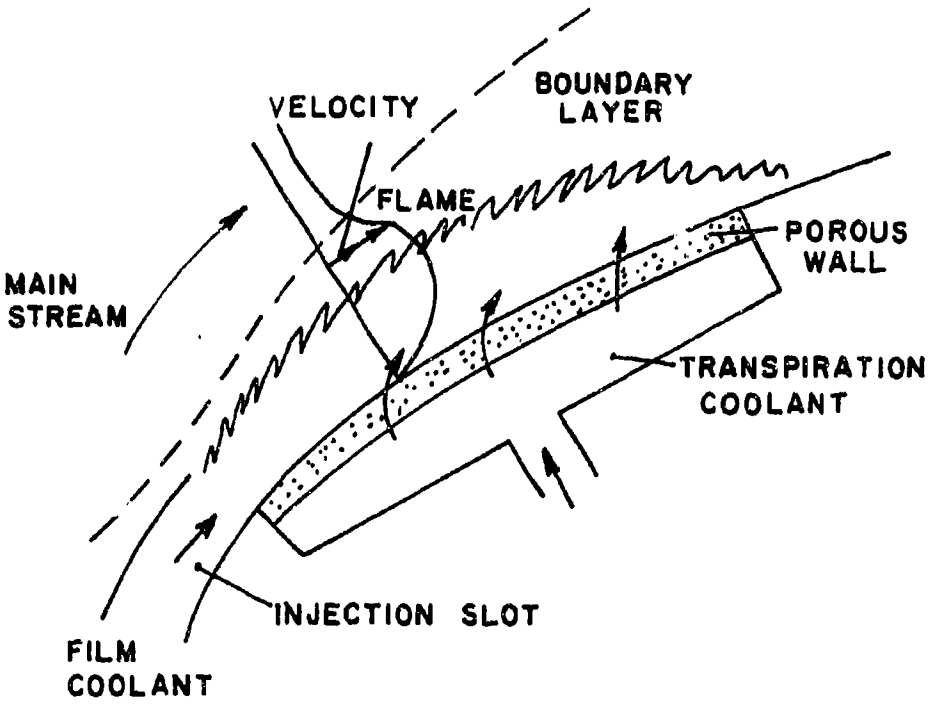

FIGURE 19 PROCESSES CONSIDERED BY SPALDING (1965)

which Spalding has tried to account for in his theory. The purpose of the unified theory was to develop a set of equations such that each term or set of terms account for one of the flow characteristics shown. The engineer could then eliminate those terms which are not necessary for the particular case he is considering. In this instance, all but those terms pertaining to film coolant flow may be eliminated from consideration.

The theory is based on two postulates. First, the profiles of velocity, temperature, and concentration are described by expressions with two main components, a boundary-layer component and a wall jet component. The boundary-layer component accounts for the momentum, heat, and mass transfer to the wall. The jet component models the effects of interaction between the coolant stream and the mainstream. The second postulate assumes that fluid is entrained into the wall layer in the same manner as in a turbulent jet.

There are two restirctions on the following development: firstly, the properties of fluid (density, viscosity, specific heat, and thermal conductivity) are constant across the boundary layer; secondly, the wall is hydrodynamically smooth.

The mathematical quantities which are of concern are defined by three integral quantities (I) and five Reynolds numbers. The three intergral properties depend on Z ($= u/u_{ms}$) or ϕ (a conserved property) as follows:

$$I_1 \equiv \int_0^1 (\rho/\rho_{ms})\, Z\, d\xi \qquad (4\text{-}19)$$

$$I_2 \equiv \int_0^1 (\rho/\rho_{ms})\, Z^2\, d\xi \qquad (4\text{-}20)$$

$$I_\phi \equiv \int_0^1 (\phi/\phi_{ms})(\rho/\rho_{ms})\, Z\, d\xi \qquad (4\text{-}21)$$

where $\xi = y/y_{ms}$, and the subscript ms stands for the mainstream quantity. These expressions may be related to the displacement thickness δ_1, the momentum thickness δ_2, and the shape factor H:

$$\delta_1/y_{ms} = 1 - I_1 \qquad (4\text{-}22)$$

$$\delta_2/y_{ms} = I_1 - I_2 \tag{4-23}$$

$$H = \delta_1/\delta_2 = (1 - I_1)/(I_1 - I_2) \tag{4-24}$$

In order to provide conservation laws in the form presented by Spalding, it is necessary to define five different Reynolds numbers:

$$Re_{ms} \equiv \rho_{ms}\, u_{ms}\, y_{ms}/\mu_{ms} \tag{4-25}$$

$$Re_2 \equiv \rho_{ms}\, u_{ms}\, \delta_2/\mu_{ms} = (I_1 - I_2)\, Re_{ms} \tag{4-26}$$

$$Re_m \equiv \int_0^{y_{ms}} (\rho u/\mu_{ms})\, dy = I_1\, Re_{ms} \tag{4-27}$$

$$Re_{max} \equiv \rho_{ms}\, u_{max}\, y_{max}/\mu_{ms} \tag{4-28}$$

$$Re_x \equiv \int_0^x (\rho_{ms}\, u_{ms}/y_{ms})\, dx \tag{4-29}$$

Using the above, the conservation laws may now be developed.

Three conservation laws, conservation of mass, momentum, and a conserved property ϕ, may now be written as first order ordinary differential equations; for conservation of mass

$$\frac{d\, Re_m}{d\, Re_x} + Re_m \frac{d(\rho w)}{d\, Re_x} = -m_{ms} + m \tag{4-30}$$

where w is the distance between adjacent streamlines in the direction parallel to the surface and normal to the flow, and m is the mass transfer rate (nondimensional) into the boundary layer through the wall:

$$m = \dot{m}''/(\rho_{ms}\, u_{ms}) \tag{4-31}$$

The quantity m_{ms} is the nondimensional rate of entrainment of mass into the boundary layer:

$$m_{ms} = \dot{m}''_{ENT}/\rho_{ms}\, u_{ms} \tag{4-32}$$

The conservation of momentum equation may be represented by:

$$\frac{d\ Re_2}{d\ Re_x} + (1 + H)\ Re_2 \frac{d\ (\ell n\ u_{ms})}{d\ Re_x} + Re_2 \frac{d\ (\ell n\ w)}{d\ Re_x} = s + m \qquad (4\text{-}33)$$

where

$$s = \frac{\tau}{(\rho_{ms}\ u_{ms}^2)} = \frac{C_f}{2} \qquad (4\text{-}34)$$

which is a measure of the shear force acting on the fluid.

The final conservation equation is the conservation of a property such as enthalpy or species concentration:

$$\frac{d}{d\ Re_x}\left(\frac{I_\phi}{I_1} Re_m\right) + \frac{I_\phi}{I_1} Re_m \frac{d\ (\ell n\ w)}{d\ Re_x} = m\ (\phi_T - \phi_{ms}) \qquad (4\text{-}35)$$

where the subscript T stands for the "transfered-substance state".

Before the three conservation equations may be solved, several more relations are necessary. The first of these is the assumed velocity distribution under uniform-density conditions:

$$Z = S^{1/2}\ u^+ + (1 + Z_E)\ (-\cos \pi\ \xi)/2 \qquad (4\text{-}36)$$

The first term of the above relates to the "law of the wall" and the second to the "law of the wake". The terminology here relates to a paper by Coles (Schlichting, 1960) in which the velocity profile was assumed to be represented by a linear combination of two universal functions, "the law of the wall" being the first, the "law of the wake" the second. In the above the shear stress term function u^+ is related to the nondimensional distance from the wall y^+, where:

$$y^+ = y(\tau\rho)^{1/2}/\mu \qquad (4\text{-}37)$$

The quantity $(1 - Z_E)$ measures the magnitude of the free-mixing-layer component of the velocity profile. The final quantity $(1 - \cos \pi\ \xi)/2$ is a correlation of empirical results.

Through a series of approximations, Spalding replaced the unknown function u^+ and obtained:

$$Z \simeq 2.5\ (s + m\ Z_E)^{1/2}\ \ell n\ \xi + Z_E + (1 - Z_E)\cdot$$

$$\cdot(\ 1 - \cos \pi\ \xi)/2 \qquad (4\text{-}38)$$

The inclusion of the mass flux term through the wall represents the shear stress component due to such a mass flux.

The second necessary relation is the mass entrainment relation, which is defined as:

$$-\ m_{ms} = \frac{3 + Z_o}{8}\ \frac{y_{ms}}{x} \qquad (4\text{-}39)$$

where Z_o is related to the velocity of the mixing layer and that of the freestream.

Now that general equations have been provided for the physical situation believed present, rather than continuing with the lengthy derivation of the theory, it will be benificial to apply Eqn. (4-30) through (4-35) to the wall jet. The mass flux through the wall is set equal to zero because the situation consideres flow only from a slot. The term $d\ (\ell n\ w)/d\ Re_x$ becomes zero if a constant width of the stream is assumed. This reduces equation (4-30) to:

$$\frac{d\ Re_m}{d\ Re_x} = -\ m_{ms} \qquad (4\text{-}40)$$

Similarly, since u_{ms} is assumed to be nearly zero for the wall jet, the $d\ (\ell n\ u_{ms})/d\ Re_x$ term may be eliminated from Eqn. (4-33) and (4-35):

$$\frac{d\ Re_2}{d\ Re_x} = s \qquad (4\text{-}41)$$

and

$$\frac{d}{d\ Re_x}\ \left(\frac{I_\phi}{I_1}\ Re_m\right) = 0 \qquad (4\text{-}42)$$

Using the above relations. Spalding showed that:

$$\frac{Re_m}{\rho\, u_s\, h_s'/\mu} \sim 1.837\, (C_2 \frac{x}{h_s'})^{1/2} \qquad (4\text{-}43)$$

where the slot height is given by h_s' and u_s represents the coolant velocity. In the case of the wall jet:

$$Re_m \sim \frac{\rho\, u_{max}\, \delta}{\mu} \qquad (4\text{-}44)$$

such that

$$\frac{u_{max}\, \delta}{u_s\, h_s'} \sim 1.837\, (C_2 \frac{x}{h_s'})^{1/2} \qquad (4\text{-}45)$$

which using an expression given by Spalding for δ yields:

$$\frac{u_{max}}{u_s} \sim 0.695\, (C_2 \frac{x}{h_s'})^{-1/2} \qquad (4\text{-}46)$$

Comparison of Eqn. (4-45) and (4-46) to those of Seban and Back (see Eqn. (4-16) and (4-17)) indicates the theory is definitly of the correct form. Experimental results presented by Spalding show that C_2 has been determined by Stratford et al. so that Eqn. (4-46) becomes:

$$\frac{u_{max}}{u_s} \sim 3.6\, (\frac{x}{h_s'})^{-1/2} \qquad (4\text{-}47)$$

The excellent agreement exhibited here encourages the use of Spalding's enthalpy flux equation:

$$\frac{h - h_{ms}}{h_s - h_{ms}} = \frac{\rho\, u_s\, h_s'/\mu}{Re_m} \frac{\frac{1}{2} - \frac{1}{\ell}}{\frac{1}{2} - \frac{n}{8} - \ell\,(1 - 0.2055n)} \qquad (4\text{-}48)$$

where $\ell = 9.94$, an empirically determined value, and n is a quantity which accounts for the fact that heat and mass are transfered faster in a free jet than is momentum. Thus, if $n = 1$, the exchange is equal,

that is, heat is transfered at the same rate as momentum. If n = 0, heat and mass transfer is assumed to be infinitely fast compared to momentum transfer. Inserting the value of ℓ = 9.94 and Eqn. (4-43) into (4-48):

$$\frac{h - h_{ms}}{h_s - h_{ms}} = \frac{3.14}{1 - 0.251\ n} \left(\frac{h'_s}{x}\right)^{1/2} \qquad (4\text{-}49)$$

where h is the enthalpy of the gas next to the wall (the gas temperature can be assumed to be very close to the wall temperature). The value on the left hand side of Eqn. (4-49) is a measure of the efficiency of the film coolant in maintaining a low wall temperature. In a latter part of this section it will be more often termed the efficiency of film cooling. Often the expression is written as follows:

$$\frac{h - h_{ms}}{h_s - h_{ms}} = \frac{c_p T - c_{p_{ms}} T_{ms}}{c_{p_s} T_s - c_{p_{ms}} T_{ms}} \qquad (4\text{-}50)$$

assuming the values of c_p are relatively close,

$$\frac{T - T_{ms}}{T_s - T_{ms}} = \frac{3.14}{1 - 0.251\ n} \left(\frac{h'_s}{x}\right)^{1/2} \qquad (4\text{-}51)$$

Since the above is the result of a semi-empirical theory, one might question the improvement over the findings of experiments and correlations such as those presented by Seban and Back (1960). The improvement lies in the relatively few unknowns in Eqn. (4-51). Rather than providing a different correlation for each mainstream and coolant velocity ratio, only a value of n need be determined to calculate the effectiveness of the film cooling wall jet.

In conclusion, the work of Glauert provides an understanding of the flow issuing from a wall jet. However, since Reynold's analogy may not be used to extend Glauert's results, empirical information is necessary to ascertain the temperature distribution. The theory of Spalding was then developed in general and applied to the specific case of the

wall jet. The previously reviewed findings of Seban and Back (1960) substantiate the theoretical predictions of Spalding.

B. 2-3) The Turbulent Film Cooling Boundary Layer Region

The investigations concerning the turbulent boundary layer region have, for the most part, been experimental and have outnumbered those for the potential core and wall jet regions. This is primarily due to the fact that the turbulent region exists over the major portion of the area protected by the film cooling blanket. A secondary reason for the interest in this region is that here the parameters of the flow will most effect the wall temperature. In the potential core region sufficient coolant exists to prevent excessive temperatures from being reached, and if the mainstream velocity is greater than the coolant velocity, the wall jet region does not exist. Since this is most often the case in combustion chambers the boundary layer region is of special importance.

The experimental investigations may be catagorized into two divisions, those with low mainstream temperatures (<700 °R) with film cooling or heating, and those with mainstream temperatures in the range of those found in gas turbines. Fortunately, division of the empirical results into these two groups eliminates many of the studies which present correlations with little physical insight. However, one such correlation of data remains (Papell and Trout, 1959) and will be discussed first in the section below. The need for a theoretical approach is dramatically evident from such a study. The work of Spalding (1965) mentioned in the previous section will be briefly extended to the situation of film cooling in the turbulent region. The results of the theory will be compared to the empirical results of Seban and Back (1962). Finally, the results of Hartnett et al. (1961) will be shown to be of the same form as those predicted by Spalding. The emphasis in this section is again placed on the theoretical approach since the conditions of interest are not adequatly covered by empirical results.

Papell and Trout (1959) were among the first investigators to study film cooling of an adiabatic flat plate. The range of conditions of their experiments is shown in Table 3.

Table 3.
Experimental Conditions
for the Study of Papell and
Trout (1959)

Mainstream Gas Temperature	520 °R to 2000 °R
Mainstream Mach Number	0.15 to 0.70
Cooling Air Temperature	540 °R to 870 °R
Cooling Air Mach Number	0.0 to 1.0
Slot Height	1/2, 1/4, 1/8, and 1/16 inches

With very little introduction as to why the efficiency of the film cooling slot should depend on any specific quantities, the authors presented a general correlation form:

$$\frac{T_{ms} - T_{aw}}{T_{ms} - T_s} = K \left[\frac{(\rho u)_s}{(\rho u)_{ms}}\right]^w \left(\frac{h'_s}{x}\right)^y \left(\frac{T_s}{T_{ms}}\right)^z \qquad (4\text{-}52)$$

where

$$\frac{T_{ms} - T_{aw}}{T_{ms} - T_s} \equiv \eta$$

Although the dependence of the efficiency on mass flow rates and slot height is evident the authors provided no reasons for the inclusion of the temperature ratio. Also absent from the analysis was a discussion of the physical reasons for organizing the components in the manner shown.

In lieu of such empirical correlations, a theoretical efficiency has been provided by Spalding's "Unified Theory". The development of a theoretical approach is of interest for two reasons: the results provide insight into the phenomena concerning the flow, and the results may more safely be extended to conditions which have not been experimentally investigated. The relation between the physical and mathematical findings have been outlined in the previous section. The only point which should be made is that the freestream velocity is no longer zero. Interaction of the freestream and the boundary layer leads to the turbulent mixing and heat transfer.

Therefore, the results of Spalding's theory for film cooling effectiveness of a turbulent boundary layer may be expressed as:

$$\frac{h_{ms} - h}{h_{ms} - h_s} = 27.02 \left(\frac{\rho_s u_s h'_s/\mu}{Re_x^{0.8}}\right) \cdot \left[\frac{\frac{1}{8} + Z_E\left(\frac{1}{4} - \frac{0.589}{t}\right) - Z_E^2\left(\frac{3}{8} - \frac{0.569}{t} + \frac{2}{t^2}\right)}{\left(\frac{1}{2} - \frac{3}{8}n + Z_E\left(\frac{1}{2} - \frac{n}{8} - \frac{1}{t} + 0.2055\frac{n}{t}\right)\right.}\right] \qquad (4\text{-}53)$$

The value of x necessary for the integration of Re_x will not be the dis-

tance from the slot exit, since the boundary layer appears to start somewhere ahead of the slot exit.

The above may be compared to the experimental work of Seban and Back (1962), for which Spalding determined $Z_E = 0.903$, $\ell = 8.77$, and $n = 0.63$ for a slot height of 1/16 inch. The bracketed term in (4-53) then becomes equal to 0.210, and (4-53) reduces to:

$$\frac{h_{ms} - h}{h_{ms} - h_s} = 5.67 \left(\frac{\rho_s u_s h'_s \mu}{Re_x^{0.8}}\right) \qquad (4\text{-}54)$$

The comparison between the theoretical and experimental efficiencies is shown in Fig. 20 as a function of $(\rho_s u_s/\rho_{ms} u_{ms})(y_{ms}/\delta_2)$, the momentum thickness. The two extreme cases of $n = 1.0$ (momentum transfer equals heat and mass transfer) and $n = 0$ (infinitely fast heat and mass transfer) are also shown in Fig. 20.

A parallel analysis by Hartnett, Birkebak, and Eckert (1961) provides a similar relation to that of Spalding. These authors proposed that the energy contained at any boundary layer cross section of the flow downstream of a slot must be equal to the energy added through the slot,

$$\dot{E}_{SLOT} = \int_0^{\delta_{BL}} \rho u c_p L (T - T_{ms}) \, dy \qquad (4\text{-}55)$$

where L is the plate width and $\dot{E}_{SLOT}$ is the energy flux. The above may be expanded to give:

$$\dot{E}_{SLOT} = \rho_{ms} u_{ms} c_p L (T_{aw} - T_{ms}) \int_0^{\delta_{BL}} \left(\frac{\rho u}{\rho_{ms} u_{ms}}\right) \left(\frac{T - T_{ms}}{T_{aw} - T_{ms}}\right) dy \qquad (4\text{-}56)$$

Experimental results from the work of the authors showed that:

$$\frac{\rho u}{\rho_{ms} u_{ms}} = \left(\frac{y}{\delta_{BL}}\right)^{1/7} \qquad (4\text{-}57)$$

Similarly, the boundary layer temperature profile was found to be:

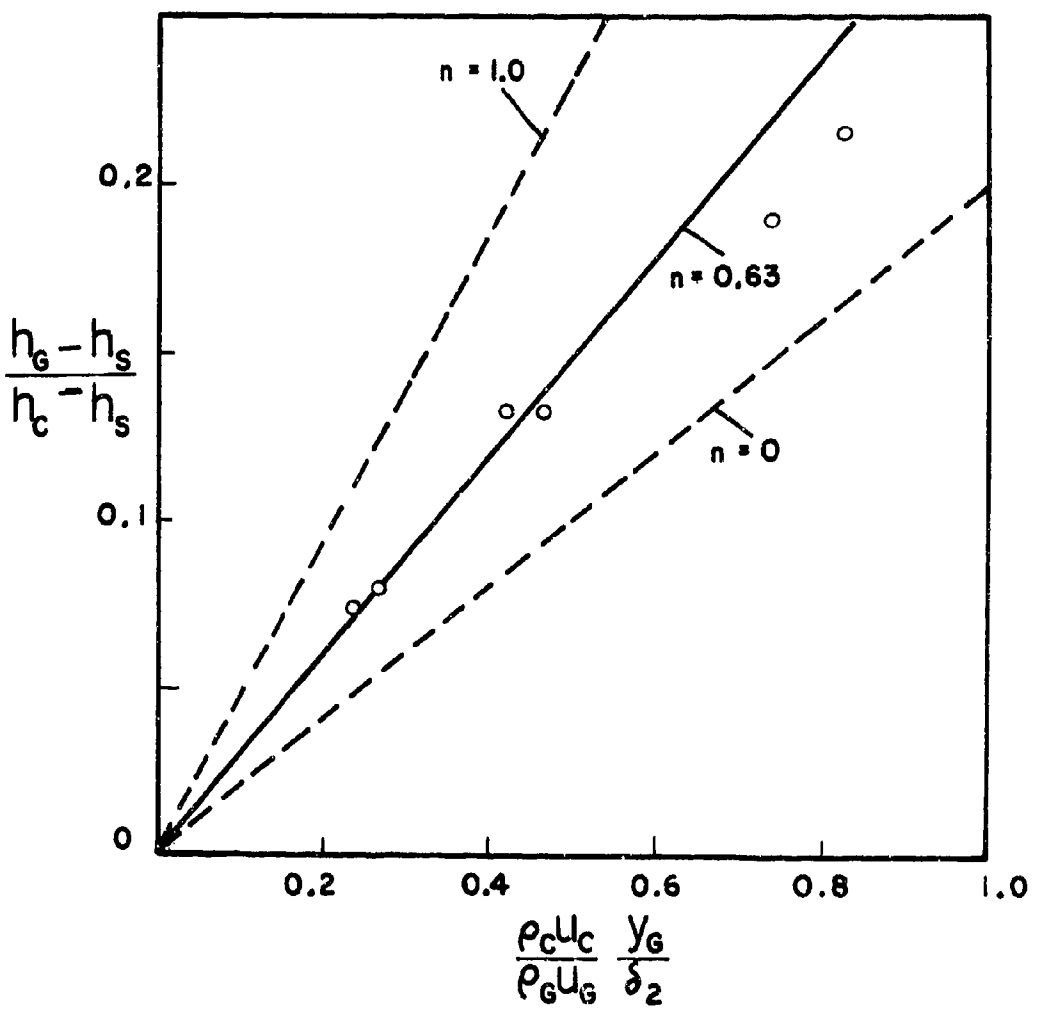

FIGURE 20 FILM-COOLING EFFECTIVENESS RELATED TO MOMENTUM THICKNESS (SPALDING, 1965)

$$\frac{T - T_{ms}}{T_{aw} - T_{ms}} - \exp\left[-C\left(\frac{y}{\delta_{BL}}\right)^{13/6}\right] = \exp\left[-C\left(\frac{y}{\delta_{BL}}\right)^{2}\right] \qquad (4\text{-}58)$$

Inserting (4-57) and (4-58) into (4-56) yields:

$$\dot{E}_{SLOT} = \rho_{ms}\, u_{ms}\, c_p\, L\, (T_{aw} - T_{ms}) \int_0^{\delta_{BL}} \left(\frac{y}{\delta_{BL}}\right)^{1/7} \exp \left[-C\left(\frac{y}{\delta_{BL}}\right)^{2}\right] dy \qquad (4\text{-}59)$$

Expanding $\exp\left[-C\,(y/\delta_{BL})^2\right]$ in a Taylor Series and retaining only the first two terms:

$$\dot{E}_{SLOT} = \rho_{ms}\, u_{ms}\, c_p\, L\, (T_{aw} - T_{ms}) \int_0^{\delta_{BL}} \left(\frac{y}{\delta_{BL}}\right)^{1/7} \left[1 - C_1'\left(\frac{y}{\delta_{BL}}\right)^2 + C_1'^2\left(\frac{y}{\delta_{BL}}\right)^4\right] dy \qquad (4\text{-}60)$$

$$= \rho_{ms}\, u_{ms}\, c_p\, L\, (T_{aw} - T_{ms})\left[7\,\delta_{BL}\left(\frac{1}{8} - \frac{C_1'}{22} + \frac{C_1'^2}{36}\right)\right] \qquad (4\text{-}61a)$$

Let

$$K_1 = 7\left(\frac{1}{8} - \frac{C_1'}{22} + \frac{C_1'^2}{36}\right) \qquad (4\text{-}61b)$$

and note that,

$$\delta_{BL} \equiv B\, X/Re_x^{1/5} \qquad (4\text{-}61c)$$

Then

$$\dot{E}_{SLOT} = K_1'\, \rho_{ms}\, u_{ms}\, c_p\, L\, X\, Re_x^{-1/5}\, (T_{aw} - T_{ms}) \qquad (4\text{-}62)$$

where

$$K_1' = BK_1$$

However, the energy flux through the slot may be expressed as:

$$\dot{E}_{SLOT} = \dot{m}_s c_p (T_s - T_{ms}) \qquad (4\text{-}63)$$

Equating Eqn. (4-62) and (4-63):

$$\dot{m}_s c_p (T_s - T_{ms}) = K_1' \rho_{ms} u_{ms} c_p L X Re_x^{-1/5} (T_{aw} - T_{ms}) \qquad (4\text{-}64)$$

But

$$\dot{m}_s \equiv \rho_s u_s h_s' L$$

Therefore, Eqn. (4-64) becomes:

$$\rho_s u_s L c_p (T_s - T_{ms}) = K_1' \rho_{ms} u_{ms} c_p L X Re_x^{-1/5} (T_{aw} - T_{ms}) \qquad (4\text{-}65)$$

Defining η as before:

$$\eta = K_1'' \left(\frac{\rho_s u_s}{\rho_{ms} u_{ms}}\right)\left(\frac{h_s'}{X}\right) Re_x^{.2} \qquad (4\text{-}66)$$

where $K_1'' = 1/K_1'$ gives:

$$\eta = K_1'' \left(\frac{\rho_s u_s}{\rho_{ms} u_{ms}}\right)^{.8}\left(\frac{h_s'}{X}\right) Re_s^{.2} \qquad (4\text{-}67)$$

for,

$$Re_s = \frac{u_s \rho_s h_s'}{\mu}$$

The value of K_1'' determined from experiment yielded:

$$\eta = 5.77 (Pr)^{2/3} (Re_s)^{.2} \left(\frac{X}{h_s'} \frac{\rho_{ms} u_{ms}}{\rho_s u_s}\right)^{-.8} \qquad (4\text{-}68)$$

which is the same form as that of Spalding (Eqn. (4-54)), except for the inclusion of the Prandtl number.

In conclusion, the necessity for a theoretical method has been

shown by reviewing the results of Papell and Trout. The theoretical analysis was the result of Spalding's "Unified Theory" which was substantiated by the results of Seban and Back. The independent development by Hartnett, Birkebak, and Eckert agrees with the form of Spalding's result. Again, the emphasis has been on the development of a theory rather than the use of correlations because of the necessity of extending the results to higher temperature application.

B. 3) Penetration Jets and Convective Cooling

Although no specific studies have been reviewed concerning penetration jets and their effect on convective cooling, two authors (Seban et al., 1957, and Papell, 1960) have investigated the efficiency of normal slot injection and the efficiency of a series of holes. Even though the conditions covered in the work of Seban et al. (1957) do not correspond to those found in typical gas turbines, their results indicate the loss in cooling effectiveness due to normal injection. The most ambitious work concerning the normal injection slot has been done by Papell (1960). Included in the study was the effect of cooling with a series of small holes injecting normally into the main flow. Due to the lack of information on penetration jets, it is believed that these results will indicate the trends of cooling efficiency due to normal injection of air.

Seban et al. (1957) studied the normal slot injection into the mainstream and its effects on film cooling efficiency. The conditions are similar to Wieghardt's studies (Stollery and El-Ehwany, 1965) for the heating of airplane wings to prevent icing. However, the reduction of efficiency for normal injection from that of tangential injection would be expected to be of the same order as for other mainstream and slot conditions. Fig. 21 indicates a drop in efficiency of up to 50% due to normal injection and should indicate the trends expected for work at higher temperatures.

Papell (1960) investigated the effect of normal injection in two systems: the slot and a series of small holes (Fig. 22). The conditions covered are outlined in Table 4. Note the fact that various angles of injection were used for the slot. The angle was varied primarily as a

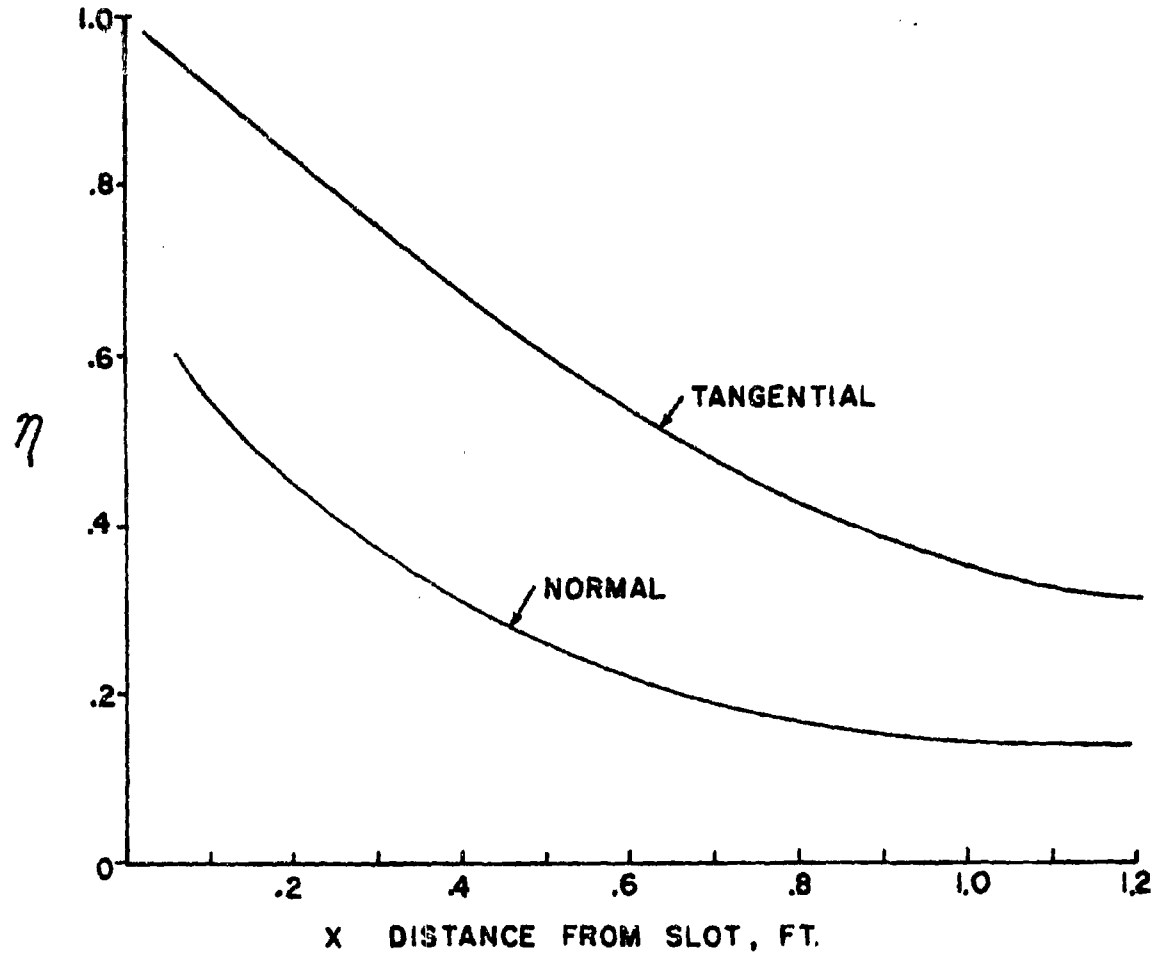

FIGURE 21 LOSS OF EFFICIENCY DUE TO NORMAL INJECTION OF COOLANT (SEBAN et al., 1957)

Table 4.
Experimental Conditions for the
Study of Papell (1960)

	Slot Configurations T_{ms} = 1500 °R T_s = 780 °R			Hole Configurations	
				Four rows of 1/4 in. holes	Two rows of 1/4 in. holes
Injection Angle	90°	80°	45°	90°	90°
Mainstream Mach Number	0.2; 0.5; 0.7	0.5	0.5	0.3; 0.6; 0.7	0.7
$\frac{u_{ms}}{u_s}$ Range	0.53 to 17.47	0.75 to 8.38	0.76 to 9.05	0.49 to 21.83	0.90 to 12.80

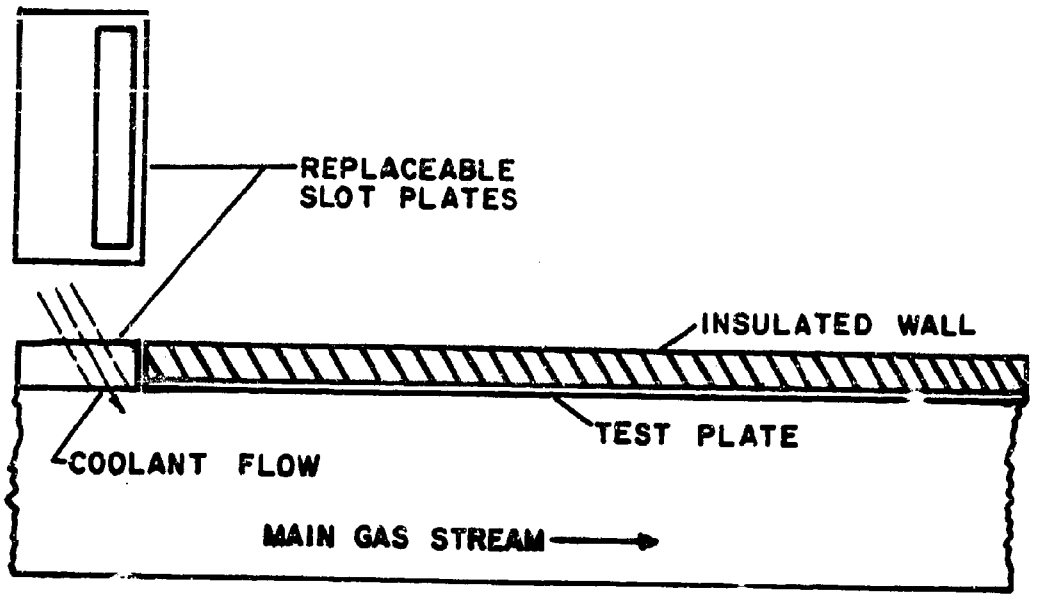

a) Slot Angle Configuration

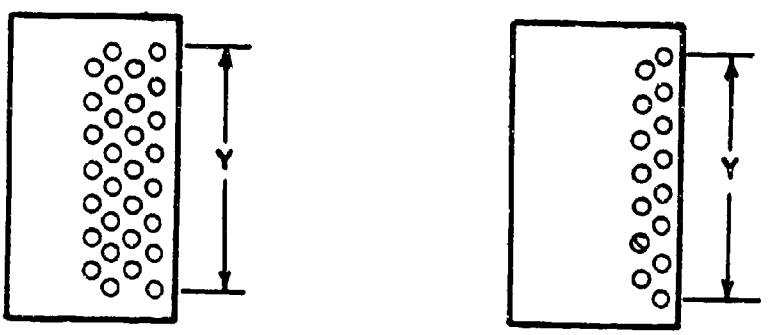

b) Normal Hole Injection Plates

FIGURE 22 EXPERIMENTAL SYSTEM AND PLATE CONFIGURATION OF PAPELL (1960)

means of confirming the physical model proposed. Papell suggested that the angle of injection and the final angle of the flow or effective injection angle i_{eff} could be related utilizing the sum of vectorial velocities of the slot and mainstream flow as shown in Fig. 23. The results from such a summation is given by:

$$i_{eff} = \tan^{-1} \frac{\sin i}{\cos i + \frac{(\rho u)_{ms}}{(\rho u)_s}} \tag{4-69}$$

In correlating the results, Papell found that the cosine of the effective angle gave the best results. The effect was then added to the film cooling correlation used in the previously cited work of Papell and Hatch (1961):

$$\log_e \eta = -\{[\frac{h_{cl}\, L\, X}{(\dot{m}\, c_p)_s} - 0.04](\frac{h'_s\, u_{ms}}{\alpha_s})^{0.125} f(\frac{u_{ms}}{u_s})\}$$

$$+ (\log_e \cos 0.8\, i_{eff}) \tag{4-70}$$

where

$$f(\frac{u_{ms}}{u_s}) = 1 + 0.4 \tan^{-1} (\frac{u_{ms}}{u_s} - 1) \text{ when } \frac{u_{ms}}{u_s} \geq 1.0$$

$$= (\frac{u_s}{u_{ms}})^{1.5 [u_s/u_{ms}) - 1]} \text{ when } \frac{u_{ms}}{u_s} \leq 1.0$$

One variation which should be noted in Eqn. (4-70) is the definition of the efficiency, η:

$$\eta \equiv \frac{T_{aw} - t_w}{T_{aw} - T_s} \tag{4-71}$$

where

$$T_{aw} \equiv t_{ms} + (Pr)_{ms}^{1/3} (T_{ms} - t_{ms})$$

and

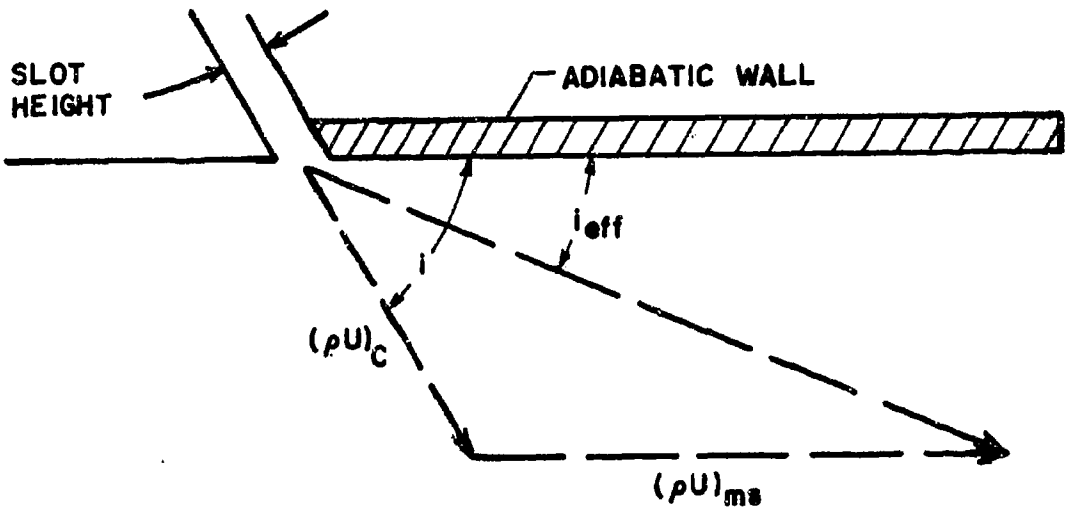

FIGURE 23 VECTORIAL SUMMATION OF VELOCITY COMPONENTS TO GIVE THE EFFECTIVE ANGLE OF INJECTION (PAPELL, 1960)

$t \equiv$ static temperature in degrees

$T \equiv$ stagnation temperature in degrees

The accuracy of this correlation was found to be approximatly 10%. Fig. 24 shows typical variations in the efficiency as the slot angle was varied with different flow rate ratios for a 1/4 inch slot. These results should indicate the variation in efficiency due to the normal injection rather than tangential injection.

An additional configuration of interest for providing coolant to the chamber walls was presented in the previously cited work of Papell (1960) and will be discussed briefly. Papell proposed the use of a series of small holes as shown in Fig. 22. As for slots, an effective slot height found empirically was used in a correlation similar to Eqn. (4-70):

$$h_s'' \equiv \frac{A_s}{L_1} \tag{4-72}$$

where

$A_s \equiv$ coolant gas flow area

$L_1 \equiv$ width of first row of holes

For $u_{ms}/u_s > 1.0$ the correlation found was:

$$\log_e \eta = -\left[\frac{h_c L X}{(\dot{m} c_p)_s} - 0.04\right] \left(\frac{h_s'' u_{ms}}{\alpha_s}\right)^{0.125} f\left(\frac{u_{ms}}{u_s}\right)$$

$$+ \log_e \cos 0.8\, i_{eff} - 0.08 \left(\frac{u_{ms}}{u_s}\right) \tag{4-73}$$

Fig. 25 illustrates typical results for the above correlation.

Typical of the early work done in the field of film cooling, other than the model presented very little physical insight is given as to why the correlation should be of the form of Eqn. (4-70) and (4-73). Therefore, the above results are to serve as an example of what the trends are expected to be for the convective contribution from pene-

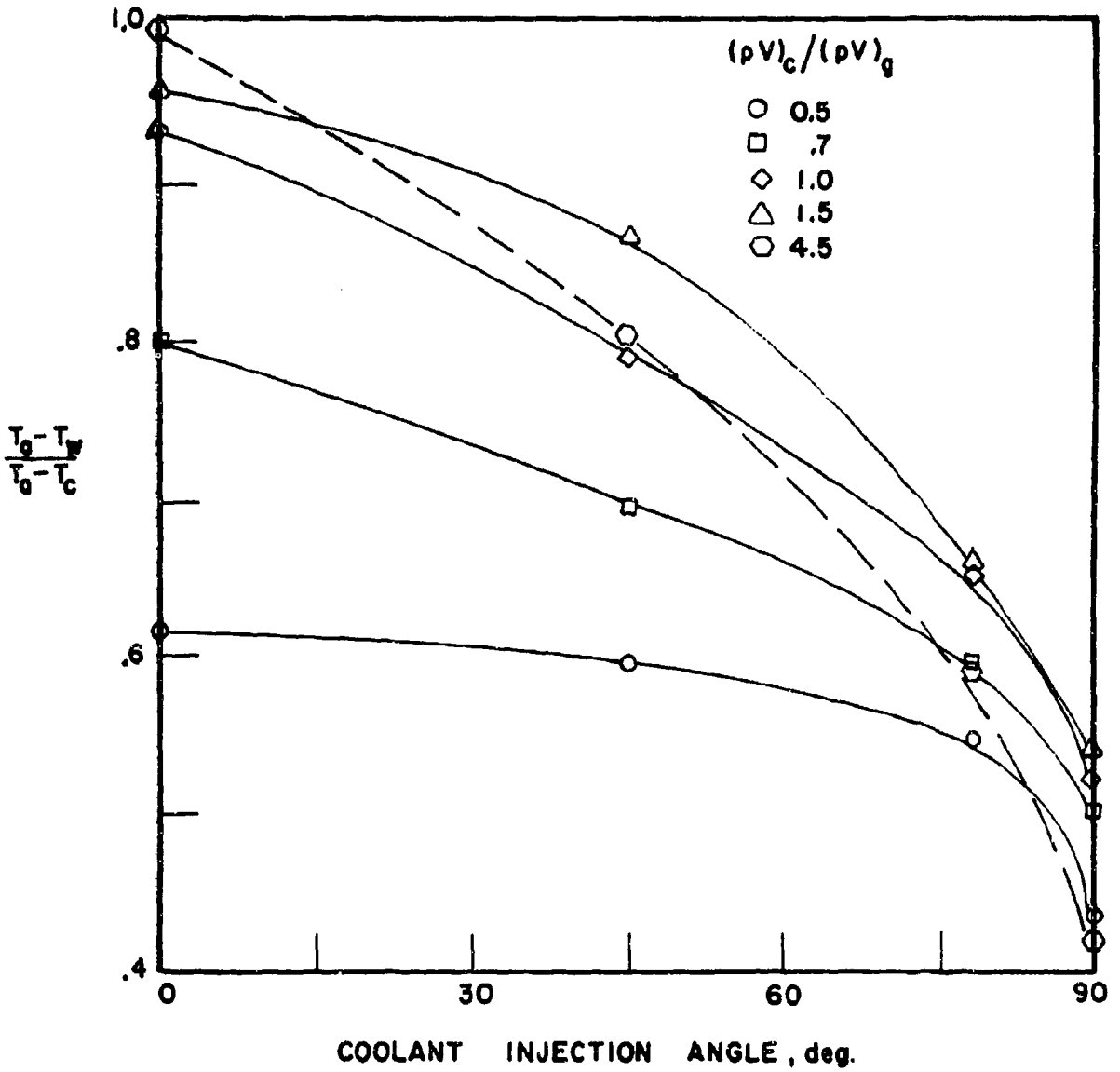

FIGURE 24 EFFECT OF VARING COOLANT INJECTION ANGLE (PAPELL, 1960)

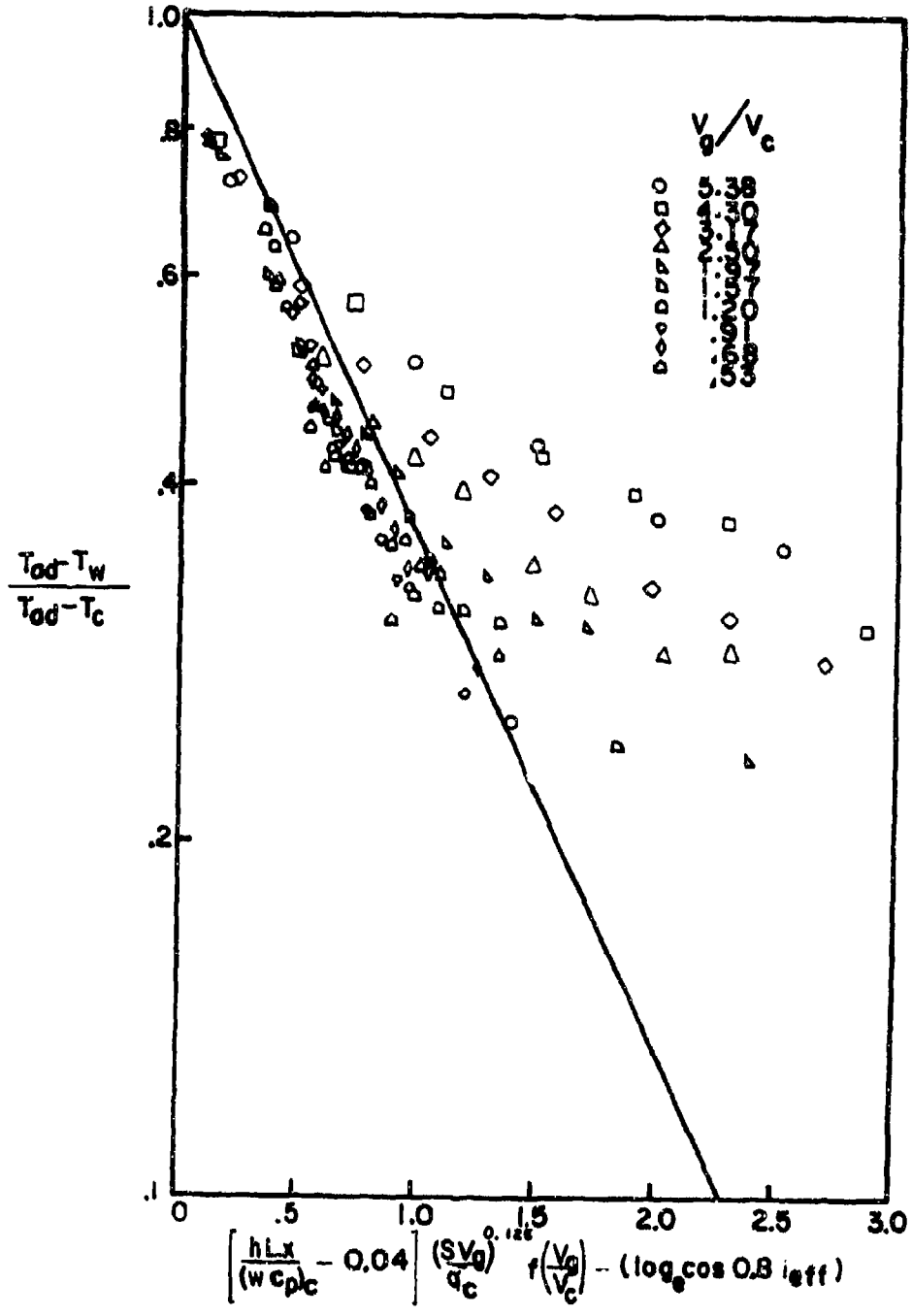

FIGURE 25 CORRELATED RESULTS USING EQUATION (4-73)

etration jets.

5. 4) Porous Walls for Transpiration Cooling

The concept of utilizing the effusion of cold annulus air through a chamber wall made of porous materials has been considered by Tipler (1955). As with film cooling, the object is to provide a sufficient air flow to form a blanket of air to protect the wall from convective heating. Although theoretical and empirical investigations have been done (Eckert and Livingood, 1953, Spalding et al., 1964, Milford and Spiers, 1961, Spalding, 1965), they will not be considered in the light of the arguments of Tipler (1955) and Milford and Spiers (1961), which are based on four reasons:

1) porous materials have a higher exposed surface area, due to the nature of the material, which makes such materials more prone to oxidation;

2) the porous material must be cooled to a lower temperature than solid walls for equal life, thus somewhat offsetting the advantages of having more continuous cooling;

3) the fine passages are prone to obstruction from impurities in the inlet air such as dust or engine oil;

4) the porosity of the material may vary appreciably within a single section of wall leading to uneven cooling and excessive wall stress. Therefore, the method of cooling by effusion has been eliminated from the present study.

C. External Convective Cooling, C_2

As for internal flow, the external convective flow is assumed to be fully developed turbulent flow and resemble flow through a pipe (Lefebvre and Herbert, 1960, Winter, 1955, and NREC (Anon., 1968)). Winter provided the following formulation of the effect of external flow with constant wall temperature:

$$C_2 = 0.0255 \left(\frac{k}{d_A}\right)^{0.214} (\rho u_A c_p)^{0.786} (T_w - T_{CA}) \qquad (4\text{-}74)$$

where the Nusselt number is:

$$\frac{h_C\, d_A}{k} = 0.025 \left(\frac{d_A\, \rho\, u_A\, c_p}{k}\right)^{0.786} \qquad (4\text{-}75)$$

and is similar to that found by Lyon and modified by Seban and Shimazaki (McAdams, 1954) for fully developed turbulent flow with constant wall flux:

$$\frac{h_C\, d_A}{k} = 5.0 + 0.025 \left(\frac{d_A\, \rho\, u_A\, c_p}{k}\right)^{0.8}$$

The factor of 5 is eliminated because it is almost negligible compared to the magnitude of the other terms. The other two formulations use studies done specifically in pipe flow.

Lefebvre and Herbert (1960) and NREC (Anon., 1968) have approached the problem is the same fashion and differ only slightly in the final outcome. The studies of fully developed turbulent pipe flow of Bialokoz and Saunders (1956) were used by Lefebvre and Herbert in the following form:

$$C_2 = 0.02 \left(\frac{k}{\mu^{0.8}}\right) \left(\frac{(\rho\, u_A)^{0.8}}{d_A^{*\,0.2}}\right) (T_w - T_{CA}) \qquad (4\text{-}76)$$

NREC (Anon., 1968) calculated C_2 with a similar relation formulated by Humble et al. (1951):

$$C_2 = 0.023 \left(\frac{k^{0.6}}{\mu^{0.4}}\right)\left(\frac{(\rho\, u_A)^{0.8}}{d_A^{*\,0.2}}\right) c_p^{0.4}\, (T_w - T_{CA}) \qquad (4\text{-}77)$$

Inspection of Eqn. (4-76) and (4-77) reveals that they differ by a factor of $(1/Pr)^{0.4}$ included in Eqn. (4-77). For air in the range of temperatures considered in gas turbines this factor ranges from 1.10 to 1.15. The relative ease of calculating either expression favors the use of the somewhat more precise value of Humble et al. The assumption that the flow is fully developed and resembles the flow inside of a pipe is deemed a reasonable approximation for the calculation of C_2.

CHAPTER V

SUMMARY AND FUTURE EFFORTS

Utilizing the superpositioning theory, each of the terms of Eqn. (2-35) have been determined as a function of the wall temperature.

$$R_1 + C_1 + K = R_3 + C_2 + R_2 \qquad (2\text{-}35)$$

These equations are summarized in Table 5.

The solution of Eqn. (2-35) is not of supreme importance at this point in the present study. Of more importance is a summary, firstly, of what has been accomplished and secondly, what terms in Table 5 need to be studied further.

In the first section of the report, the phenomena present in the combustion chamber were presented through the use of the conservation equations (Eqn. (2-1) - (2-4)). A formal solution utilizing these equations was shown to become an intractable problem in the presence of the velocity and concentration profiles existing in the chamber. The theory of radiative transport was then developed to yield the approximation made by Einstein (1963). The superpositioning approximation was thus shown to be the only alternative to an exact solution.

The third chapter of the report was concerned with the radiative terms present in the chamber and the analysis of each. The approximate solution necessary for predicting flame radiation on a one and two dimensional basis was reviewed. The unfortunate dependence of the calculation on the empirical emissivities was also revealed. This field will most likely have enjoyed a great deal of research since 1966. One objective proposed would be to establish theoretical reasoning for luminous emissivity values; however, unless a scheme for predicting the distribution of carbon particles has been provided in the literature or can be deduced, this endeavor will be fruitless. Additional research

Table 5.

Heat Transfer Components

$$R_l = \left(\frac{1 + \epsilon_w}{2}\right) \epsilon_f \sigma_{SB} T_f^{1.5} (T_f^{2.5} - T_w^{2.5}) \qquad (3\text{-}5)$$

or

$$R_l = \frac{4 \sigma_{SB} (1 + \alpha_w)}{2} \sum_{\substack{\text{ALL FLAME} \\ \text{POSITIONS}}} \left(\Gamma_{mean} P_G \left(\frac{\partial \epsilon_f}{\partial P_G \Sigma}\right)_o \cdot \right.$$

$$\left. \cdot \Delta X_f A_{X_{CS}} F_{fw} (T_f^4 - T_w^4)\right] \qquad (3\text{-}19)$$

$$C_l = 0.020 \frac{\lambda}{\mu^{0.8}} \left(\frac{Q_p}{A_p}\right)^{0.8} \frac{(T_g - T_w)}{d_p^{*0.2}} \qquad (4\text{-}2)$$

$$C_{l_{PC}} = h_c A (T_w - T_s) \qquad (4\text{-}3)$$

$$C_{l_{MJ}} = h_c A (T_{ms} - T_w)$$

where

$$T_w = T_{ms} + (T_s - T_{ms}) \frac{3.14}{1 - .025 \ln} \left(\frac{h_s'}{X}\right)^{1/2} \qquad (4\text{-}51)$$

$$C_{l_{TBL}} = h_c A (T_{ms} - T_w)$$

where

$$T_w = T_{ms} + (T_s - T_{ms}) \, 5.67 \frac{(\rho_s u_s h_s'/\mu)}{Re_X^{0.8}}$$

$$K = K_f \frac{\partial T}{\partial X_f} \qquad (2\text{-}34)$$

$$R_2 = \sigma_{SB}\,\varepsilon_w \sum_{\substack{\text{ALL WALL}\\ \text{POSITIONS}}} F_{dA_1-dA_2}\,\Gamma\,(T_{w_1}^4 - T_{w_2}^4) \qquad (3\text{-}34)$$

$$R_2 = R_{w\text{-}c}\,\sigma_{SB}\,(T_w^4 - T_{CA}^4)$$

$$C_2 = 0.023\left(\frac{k^{0.6}}{\mu^{0.4}}\right)\left(\frac{(\rho\, u_A^{0.8})}{d_A^{*0.2}}\right) c_p^{0.4}\,(T_w - T_{CA}) \qquad (4\text{-}77)$$

will be conducted to determine the advancements and possibilities of utilizing the theory of radiative transport in the combustion chamber. In conclusion, advancements in determining flame emissivities and the appplication of the radiative transport theory appear to be the only steps short of solving the more exact integro-differential equation of energy conservation.

As Lefebvre and Herbert (1960) pointed out, the convective contribustion in the primary zone is poorly understood. Sufficient knowledge of the recirculation flows in the primary zone is not available for a more realistic analysis to be considered (see Hammond and Mellor, 1971). Hopefully, the lack of accuracy in determining the profiles in this region will not be harmful because the annulus flow is the coldest around this region. Thus, the wall temperature rise should be limited. Judging from the numerous investigations of film cooling, this area will hopefully provide useful advances especially concerning theoretical approaches such as Spalding's (1965). Finally, as mentioned in the section on external cooling, the analogy between the external flow and the flow over a flat plate is believed to be accurate. Therefore, if advancements are to be made, the analysis of convective cooling and heating will be the most likely fields for these advances.

Although the second chapter has seemingly ruled out the more exact approach, the approach of solving the conservation equations will be considered in the future. At this time, the possible paths for analysis appear to lead in two directions: 1) the exact approach through solution to the conservation equations, and 2) approximate methods such as the theory of superpositioning. The literature review of articles written since 1966 should provide intelligent direction to the most accurate approach possible.

LIST OF REFERENCES

Anderson, R. and Mellor, A. M., 1971, An Investigation of Gas Turbine Combustors with High Inlet Air Temperatures, Second Annual Report, Part III; Experimental Developments, TM-71-3, Jet Propulsion Center, Purdue University, Lafayette, Indiana, TACOM Report No. 11322.

Anon., 1968, Computer Program for the Analysis of Annular Combustors, Volume I: Calculation Procedures; Volume II: Operating Mannual, Northern Research Eng. Corp. Reports No. 1111-1 and 1111-2, (NASA CR 72374, 72375).

Aref, M. N. and Sakkal, M. F., 1962, The Emission of Radiant Heat from Small Scale Pulverized-Coal Flames, A.S.M.E. Paper No. 63-HT-5.

Back, L. H. and Seban, R. A., 1962, Effectiveness and Heat Transfer for a Turbulent Boundary Layer with Tangential Injection and Variable Free-Stream Velocity, Journal of Heat Transfer, ASME Series C, 84, 2, 235.

Beer, J. M. and Claus, I. J., 1962, The 'Traversing' Method of Radiation Measurements in Luminous Flames, Journal of the Institute of Fuel, 35, 261, 437.

Bialokoz, J. E. and Saunders, O. A., 1956, Heat Transfer in Pipe Flow at High Speeds, Procadings of the Instn. of Mechanical Engrs., London, 170, 389.

Bird, R. B., Stewart, W. E. and Lightfoot, E. M., 1960, Transport Phenomena, John Wiley and Sons, Inc., New York.

Cess, R. D., 1964, The Interaction of Thermal Radiation with Conduction and Convection Heat Transfer, Advances in Heat Transfer, Academic Press, 1, 1.

Chin, J. H., Skirvin, S. C., Hayes, L. E. and Burggrat, F., 1961, I. Film Cooling with Multiple Slots and Louvers, II. Multiple Rows of Descrete Louvers, Journal of Heat Transfer A.S.M.E. Series C, 83, 3, 281.

Chin, J. H., Skirvin, S. C., Hayes, L. E. and Silver, A. H., 1958, Adiabatic Wall Temperatures Downstream of a Single, Tangential Injection Slot, A.S.M.E. Papers A, 58-A-107.

Eckert, E. R. G. and Livingood, J. N. B., 1953, Comparison of Effectiveness of Convection-, Transpiration-, and Film-Cooling Methods with Air as Coolant, NACA TN D-3010.

Einstein, T. H., 1963, Radiant Heat Transfer to Absorbing Gases Enclosed Between Parallel Flat Plates with Flow and Conduction, NASA TR-154.

Glauert, M. B., 1956, The Wall Jet, Journal of Fluid Mechanics, 1, 4.

Guy, A. G., 1959, Elements of Physical Metallury, Addison-Wesley, 278.

Hamilton, D. C. and Morgan, W. R., 1952, Radiation Exchange Configuration Factors, NACA TN 2836.

Hammond, D. C. and Mellor, A. M., 1970a, An Investigation of Gas Turbine Combustors with High Inlet Air Temperatures, First Annual Report: Part 1: Analytical Developments, TM-70-2, Jet Propulsion Center, Purdue University, Lafayette, Indiana.

Hammond, D. C. and Mellor, A. M., 1970b, A Preliminary Investigation of Gas Turbine Combustor Modelling, Combustion Science and Technology, 2, 67.

Hammond, D. C. and Mellor, A. M., 1971, An Investigation of Gas Turbine Combustor with High Inlet Air Temperatures, Second Annual Report; Part 1: Combustion Modelling, TM-71-1, Jet Propulsion Center, Purdue University, Lafayette, Indiana, TACOM Report No. 11321.

Hartnett, J. P., Birkebak, R. C., and Eckert, E. R. G., 1961, Velocity Distributions, Temperature Distributions, Effectiveness, and Heat Transfer for Air Injected Through a Tangential Slot into a Turbulent Boundary Layer, Journal of Heat Transfer, ASME Series C, 83, 3, 293,

Hatch, J. E. and Papell, S. S., 1961, Use of a Theoretical Flow Model to Correlate Data for Film Cooling or Heating an Adiabatic Wall by Tangential Injection of Gases of Different Fluid Properties, NASA TN D-130.

Hiett, G. F. and Powell, G. F., 1962, Three-Dimensional Probe for Investigation of Flow Patterns, The Engineer, 213, 1, 165.

Howell, J. R. and Siegel, R., 1969, Thermal Radiation Heat Transfer, Vol. II. Radiation Exchange Between Surfaces and Enclosures, NASA SP-164.

Humble, L. V., Lowdermilk, W. H., and Desmond, L. E., 1951, Measurements of Average Heat Transfer and Friction Coefficients for Subsonic Flow of Air in Smooth Tubes at High Surface and Fluid Temperature, NACA TR 1020.

Lefebvre, A. H. and Herbert, M. V., 1960, Heat-Transfer Processes in Gas-Turbine Combustion Chambers, Proceedings of the Instn. of Mechanical Engrs., London, 174, 12, 463.

Lefebvre, A. H., 1965, Progress and Problems in Gas-Turbine Combustion, Tenth Symposium on Combustion, pp. 1129-1137.

McAdams, W. H., 1954, Heat Transmission, McGraw-Hill, New York.

Milford, C. M. and Spiers, D. N., 1962, An Investigation into Film Cooling by Slots, International Developments in Heat Transfer, ASME Part IV, Section A, No. 79.

Papell, S. S. and Trout, A. M., 1959, Experimental Investigation of Air Film Cooling Applied to an Adiabatic Wall by Means of An Axially Discharging Slot, NASA TN D-9.

Papell, S. S., 1960, Effect on Gaseous Film Cooling of Coolant Injection Through Angled Slots and Normal Holes, NASA TN D-299.

Sato, R., Matsumoto, R., Ueda, K., and Ohira, K., 1962, Radiant Heat Transfer from Luminous Flames, Bulletin of Japanese Society of Mechanical Engrs. 5, 17, 117.

Schlichting, H., 1960, Boundary Layer Theory, McGraw-Hill, New York.

Seban, R. A., Chan, H. W. and Scesa, S., 1957, Heat Transfer to a Turbulent Boundary Layer Downstream of an Injection Slot, ASME Series A Papers, 57-A-36.

Seban, R. A. and Back, L. H., 1962, Velocity and Temperature Profiles in Turbulent Boundary Layers with Tangential Injection, Journal of Heat Transfer, ASME Series C, 84, 1, 45.

Seban, R. A. and Back, L. H., 1960, Velocity and Temperature Profiles in a Wall Jet, International Journal of Heat and Mass Transfer, 3, 255.

Seban, R. A., 1960, Heat Transfer and Effectiveness for a Turbulent Boundary Layer with Tangential Fluid Injection, Journal of Heat Transfer, ASME Series C, 82, 303.

Spalding, D. B., 1965, A Unified Theory of Friction, Heat Transfer and Mass Transfer in the Turbulent Boundary Layer and Wall Jet, ARC CP. No. 829.

Spalding, D. B., Auslander, D. M. and Sundaram, T. R., 1964, The Calculation of Heat and Mass Transfer Through the Turbulent Boundary Layer on a Flat Plate at High Mach Numbers, with and without Chemical Reaction, Supersonic Flow, Chemical Processes, and Radiative Transfer, MacMillan, New York.

Sparrow, E. M. and Cess, R. D., 1966, Radiation Heat Transfer, Brooks/Cole, Belmont, California.

Stollery, J. L. and El-Ehwany, A. A. M., 1965, A Note on the Use of a Boundary-Layer Model for Correlating Film-Cooling Data, International Journal of Heat and Mass Transfer, 8, 55.

Stull, R. V. and Plass, G. N., 1960, Emissivity of Dispersed Carbon Particles, Journal of the Optical Society of America, 50, 2, 121.

Thring, M. W., Foster, P. J., McGrath, I. A., and Ashton, J. S., 1962, Prediction of the Emissivity of Hydrocarbon Flames, International Developments in Heat Transfer, Boulder, Colorado, 796.

Tipler, W., 1955, Combustion Chambers and Control of the Temperature at which They Operate, The Inst. of Mech. Engrs. and A.S.M.E. Joint Conference on Combustion, London, 362.

Viskanta, R., 1966, Radiation Transfer and Interaction of Convection with Radiation Heat Transfer, Advances in Heat Transfer, Academic, New York, 175.

Weeks, D. I. and Saunders, O. A., 1958, Some Studies of Radiating Flames in a Small Gas Turbine Type Combustion Chamber, Journal of the Institute of Fuel, 31, 247.

Winter, E. F., 1955, Heat Transfer Conditions at the Flame Tube Walls of an Aero Gas Turbine Combustion Chamber, Fuel, 34, 409.